Erasmus Mundus Master in Membrane Engineering 2012 - 2014

FINAL MASTER PROJECT

3D structuration of MOF layers for gas sensors enhancement and its application in microreactors

Abstract "In order to integrate ZIF-8 layers in the fabrication of microdevices and membrane, ZIF-8 layer synthesis was conducted on silicon and polymer based supports. The synthesis of ZIF-8 layer was conducted in room temperature by repeated immersion of supports in the precursor solution.

The synthesis method was compatible to the fabrication of ZIF-8 layer based microsensors and micro preconcentrator. The fabrication of free-standing micromembrane was not achieved. Study of PBI/ZIF-8 composite membrane synthesis has obtained promising results."

Cheryl Maria Karman

June 24th 2014

Supervisors: Dr. Reyes Mallada

Dr. Miguel Urbiztondo

Acknowledgement

I would like to thank Dr Reyes Mallada as the main supervisor of this project, for her support, guidance, ideas and suggestions from the beginning until the crucial moments of completing the experiments. Also I would like to thank Dr Miguel Urbitzondo as co-supervisor for his inputs and suggestions. Not to forget Dr Ismael Pellejero for his help during the research project, especially for teaching me how to work in the clean room (UV lithography, RIE, and profilemeter utilization) and the device preliminary trials. I would like to give thanks to Dr. Carlos Cuestas Ayllón for teaching me how to use the Scanning Electron Microscopy.

I also am grateful for the opportunity given by the EM3E Consortium to be a part of the the master program. I also appreciate all the help, suggestions, teaching and training given by all of my colleagues and professors at Institute of Nanotechnology Aragon, Spain.

"*The EM3E Master is an Education Programme supported by the European Commision, the European Membrane Society (EMS), the European Membrane House (EMH), and a large international network of industrial companies, research centers and universities*" (www.em3e.eu)

DISCLAMER

EN - This project has been funded with support from the European Commission. This publication reflects the views only of the author, and the Commission cannot be held responsible for any use which may be made of the information contained therein.

BG - Този проект е финансиран с подкрепата на Европейската комисия.Тази публикация отразява само личните виждания на нейния автор и от Комисията не може да бъде търсена отговорност за използването на съдържащата се в нея информация.

CS - Tento projekt byl realizován za finanční podpory Evropské unie. Za obsah publikací odpovídá výlučně autor. Publikace nereprezentují názory Evropské komise a Evropská komise neodpovídá za použití informací, jež jsou jejich obsahem.

DA - Dette projekt er finansieret med støtte fra Europa-Kommissionen. Denne publikation forpligter kun forfatteren, og Kommissionen kan ikke drages til ansvar for brug af oplysningerne heri.

DE - Dieses Projekt wurde mit Unterstützung der Europäischen Kommission finanziert. Die Verantwortung für den Inhalt dieser Veröffentlichung trägt allein der Verfasser; die Kommission haftet nicht für die weitere Verwendung der darin enthaltenen Angaben.

ΕΛ - Το σχέδιο αυτό χρηματοδοτήθηκε με την υποστήριξη της Ευρωπαϊκής Επιτροπής. Η παρούσα δημοσίευση δεσμεύει μόνο τον συντάκη της και η Επιτροπή δεν ευθύνεται για τυχόν χρήση των πληροφοριών που περιέχονται σε αυτήν.

ES - El presente proyecto ha sido financiado con el apoyo de la Comisión Europea. Esta publicación es responsabilidad exclusiva de su autor. La Comisión no es responsable del uso que pueda hacerse de la información aquí difundida.

"*The EM3E Master is an Education Programme supported by the European Commision, the European Membrane Society (EMS), the European Membrane House (EMH), and a large international network of industrial companies, research centers and universities*" (www.em3e.eu)

ET - Projekti on rahaliselt toetanud Euroopa Komisjon. Publikatsiooni sisu peegeldab autori seisukohti ja Euroopa Komisjon ei ole vastutav selles sisalduva informatsiooni kasutamise eest.

FI - Hanke on rahoitettu Euroopan komission tuella. Tästä julkaisusta (tiedotteesta) vastaa ainoastaan sen laatija, eikä komissio ole vastuussa siihen sisältyvien tietojen mahdollisesta käytöstä.

FR - Ce projet a été financé avec le soutien de la Commission européenne. Cette publication (communication) n'engage que son auteur et la Commission n'est pas responsable de l'usage qui pourrait être fait des informations qui y sont contenues.

GA - Maoiníodh an tionscadal seo le tacaíocht ón gCoimisiún Eorpach. Tuairimí an údair amháin atá san fhoilseachán [scéala] seo, agus ní bheidh an Coimisiún freagrach as aon úsáid a d'fhéadfaí a bhaint as an eolas atá ann.

HU - Az Európai Bizottság támogatást nyújtott ennek a projektnek a költségeihez. Ez a kiadvány (közlemény) a szerzõ nézeteit tükrözi, és az Európai Bizottság nem tehetõ felelõssé az abban foglaltak bárminemû felhasználásért.

IT - Il presente progetto è finanziato con il sostegno della Commissione europea. L'autore è il solo responsabile di questa pubblicazione (comunicazione) e la Commissione declina ogni responsabilità sull'uso che potrà essere fatto delle informazioni in essa contenute.

NL - Dit project werd gefinancierd met de steun van de Europese Commissie. De verantwoordelijkheid voor deze publicatie (mededeling) ligt uitsluitend bij de auteur; de Commissie kan niet aansprakelijk worden gesteld voor het gebruik van de informatie die erin is vervat.

"*The EM3E Master is an Education Programme supported by the European Commision, the European Membrane Society (EMS), the European Membrane House (EMH), and a large international network of industrial companies, research centers and universities*" (www.em3e.eu)

LT - Šis projektas finansuojamas remiant Europos Komisijai. Šis leidinys [pranešimas] atspindi tik autoriaus požiūrį, todėl Komisija negali būti laikoma atsakinga už bet kokį jame pateikiamos informacijos naudojimą.

LV - Šis projekts tika finansēts ar Eiropas Komisijas atbalstu. Šī publikācija [paziņojums] atspoguļo vienīgi autora uzskatus, un Komisijai nevar uzlikt atbildību par tajā ietvertās informācijas jebkuru iespējamo izlietojumu.

MT - Dan il-proġett ġie finanzjat bl-għajnuna tal-Kummissjoni Ewropea. Din il-publikazzjoni tirrifletti (Dan il-komunikat jirrifletti) l-opinjonijiet ta' l-awtur biss, u l-Kummissjoni ma tistax tinżamm responsabbli għal kull tip ta' uzu li jista' jsir mill-informazzjoni li tinsab fiha (fih).

PL - Ten projekt został zrealizowany przy wsparciu finansowym Komisji Europejskiej. Projekt lub publikacja odzwierciedlają jedynie stanowisko ich autora i Komisja Europejska nie ponosi odpowiedzialności za umieszczoną w niej zawartość merytoryczną.

PT - Projecto financiado com o apoio da Comissão Europeia. A informação contida nesta publicação (comunicação) vincula exclusivamente o autor, não sendo a Comissão responsável pela utilização que dela possa ser feita.

RO - Acest proiect a fost finanţat cu sprijinul Comisiei Europene.<0}Această publicaţie (comunicare) reflectă numai punctul de vedere al autorului şi Comisia nu este responsabilă pentru eventuala utilizare a informaţiilor pe care le conţine.

SK -Tento projekt bol financovaný s podporou Európskej Komisie. Táto publikácia (dokument) reprezentuje výlučne názor autora a Komisia nezodpovedá za akékoľvek použitie informácií obsiahnutých v tejto publikácii (dokumente).
SL - Izvedba tega projekta je financirana s strani Evropske komisije. Vsebina publikacije (komunikacije) je izključno odgovornost avtorja in v nobenem primeru ne predstavlja stališč Evropske komisije.

"*The EM3E Master is an Education Programme supported by the European Commision, the European Membrane Society (EMS), the European Membrane House (EMH), and a large international network of industrial companies, research centers and universities*" (www.em3e.eu)

SV - Projektet genomförs med ekonomiskt stöd från Europeiska kommissionen. För uppgifterna i denna publikation (som är ett meddelande) ansvarar endast upphovsmannen. Europeiska kommissionen tar inget ansvar för hur dessa uppgifter kan komma att användas

"*The EM3E Master is an Education Programme supported by the European Commision, the European Membrane Society (EMS), the European Membrane House (EMH), and a large international network of industrial companies, research centers and universities*" (www.em3e.eu)

Contents

Figures

Tables

Equation

Abstract

In order to integrate ZIF-8 layers in the fabrication of microdevices and membrane, ZIF-8 layer synthesis was conducted on silicon and polymer based supports. The synthesis of ZIF-8 layer was conducted in room temperature by repeated immersion of supports in the precursor solution.

The synthesis method was compatible to the fabrication of ZIF-8 layer based microsensors and micro preconcentrator. The fabrication of free-standing micromembrane was not achieved. Study of PBI/ZIF-8 composite membrane synthesis has obtained promising results.

Resumen

En este trabajo se han sintetizado capas de ZIF-8 sobre soportes de silicio y poliméros por su posterior integration en microdispositivos. La síntesis de la capa ZIF-8 se produjo a temperatura ambiente mediante la inmersión repetida de las bases en la solución precursora.

El método de síntesis fue compatible con la fabricación de micro membranas autosoportadas no se consiguió. En el estudio del compuesto PBI/ZIF-8 para síntesis de membranas asimetricas se han obtenido resultados muy prometedores.

1. Introduction

1.1 Microporous materials in the micro scale

Microsystems have been known to have many advantages compared to the classical big-scale chemical industry and production, especially by utilization of fewer raw materials and production of less waste and side products.[1] Micro reactors for example, have higher mass and heat transfer rate, so that it would improve the conversion and selectivity of the reactions.[2] The other features of micro technology which could be taken into account are its lower consumption of energy, higher surface-to-volume ratio, shorter response times, safer operation, portability and lower unit cost.[3]

Porous materials have been considered important in many applications, such as catalysis, membrane separation, gas adsorption and storage, etc.[4] Microporous materials in particular, those which have the pore diameter less than 2 nm, have been investigated and incorporated in micro devices, such as micro reactors, micro sensors, micro electronics, microelectromechanical systems (MEMS), micro membranes and micro preconcentrator.[5] Zeolite is one of microporous materials which is vastly applied for micro systems shown in Figure 1[6], especially in the areas of gas and liquid processing and controlled permeation or diffusion.

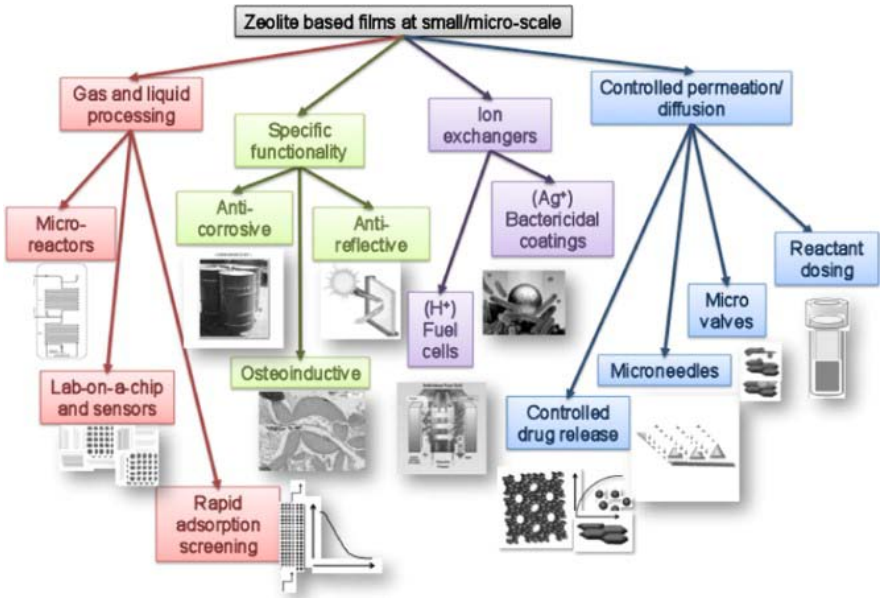

Figure 1 Diagram of zeolite films applications in the micro-scale[6]

One example of a type of zeolites which is used as micro preconcentrator to detect nitro-aromatic compounds is silicon micro pillars or micro cavities filled with DAY zeolite [7] shown in Figure 2. Beside zeolites, carbon-based materials as conventional adsorbents have been utilized to build micro preconcentrators. Pijolat et al. [8] applied carbon nano powders in porous silicon and Blanco et al. [9] microporous activated carbons, for the fabrication of micro preconcentrators used to detect benzene vapors.

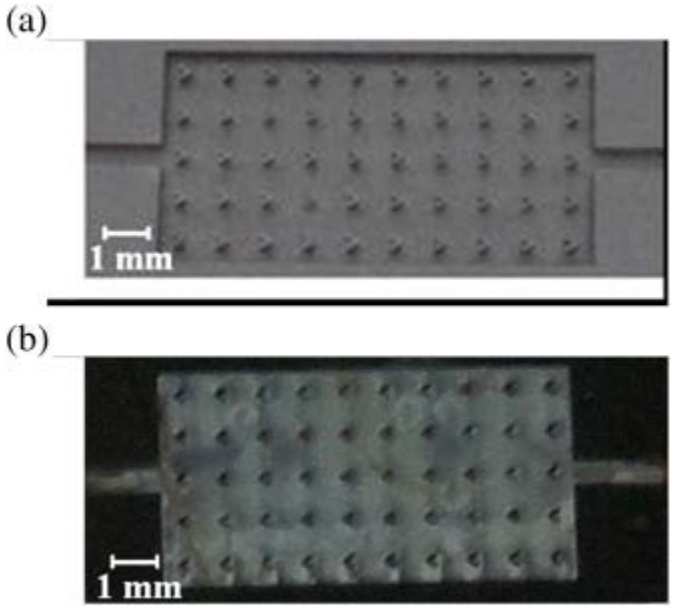

Figure 2 Silicon micro preconcentrator ((a) micro pillars, (b) micro cavities) filled with DAY zeolite [7]

In the area of micro membrane, zeolites such as SIL-1 and ZSM-5 have been extensively investigated for gas separation applications, such as benzene/air and hexane/air separation experimented by Leung et al.[10] and Coronas et al.[11] Moreover, as reported by Pellejero et al.[3], the advantage of miniaturizing zeolite membrane was the ability to produce self-standing or self-supported micro membrane which could enhance the permeance of the membrane due to exclusion of the mass transfer resistance of membrane supports.

1.2 Metal – Organic Framework

Metal – organic framework (MOF) is a considerably new class of highly porous material which structure is a crystalline framework that consists of metal cations or nodes (clusters of cations) connected by organic linkers or ligands.[12] The structure of a type of MOF (SURMOF-2) is given in Figure 3, with a composition of Zn^{2+} or Cu^{2+} dimers as metal nodes and various dicarboxylate groups as the organic ligand.

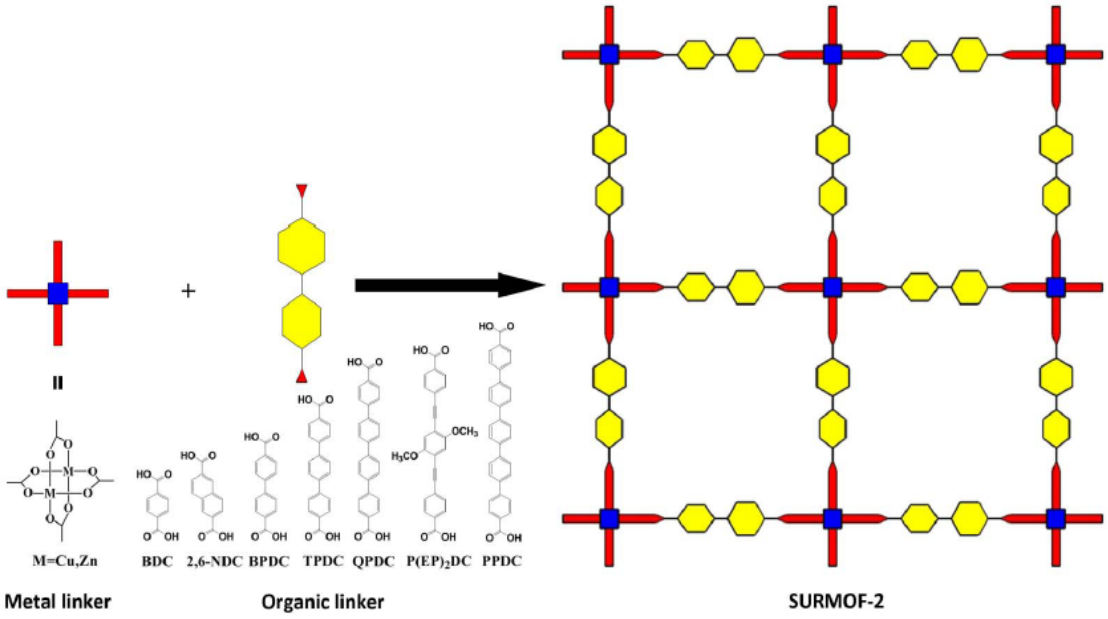

Figure 3 Schematic representation of SURMOF-2 structure consisting of metal nodes and organic ligand[13]

MOFs are often compared to zeolites as both materials share same properties, such as large internal surface areas, extensive porosity, and high degree of crystallinity. Therefore, they are applicable in fields such as gas storage and separation, and catalysis.[12] Nevertheless, compared to zeolites, MOFs have an advantage in terms of tunability[14] and mild synthesis conditions which offers better compatibility with micro devices fabrication.[2]

MOFs' pore sizes and chemical properties are tunable due to the vast types of nodes and ligands which can be connected to form different structures. Almost all metal elements, from

alkalines (Ca, Mg) to transition metals (Sc, Ti, ..., Zn), p metals (Al, Ga, In) and lanthanides can be chosen as metal nodes materials. As for organic ligands, aliphatic and aromatic compounds associated with functional groups such as carboxylates, phosphonates, sulphonates, imidazolates, amides, amines, pyridyls and nitriles, are involved in the synthesis of MOFs. The tunability of MOFs is added by the possibility of ligands functionalization with organic groups. This can provide modification of MOFs' properties (pore size, adsorption ability, spesific interaction with some molecules, etc) while maintaining the structure of the framework.[4]

MOFs also hold more potential properties compared to other microporous materials, including luminescence effect of conjugated organic ligands, structure flexibility due to host-guest interaction and change of environment conditions, charge transfer (from metal to ligand and vice versa), thermal stability relative to polymers, electronic and conducting properties, and pH stability. Therefore an extended list of applications can be conducted with MOFs, for example sensor application for chemicals detection, ion conducting membranes, drug delivery, and chemicals separation.[14]

MOF thin films

Development of MOF thin films started by the emergence of Hermes et al.[15] publication of MOF-5 films deposition on a Au substrate in 2005, followed by other types of MOFs, such as HKUST-1 and $Zn_2(bdc)_2(dabco)$.[4]

The deposition of continous and well-intergrown films can be conducted by several methods of synthesis which are generally divided into two types; direct synthesis and secondary growth. Direct synthesis involves direct immersion of the supports in the MOF precursor solution, without previously attaching any crystals on the surface (without seeding process). Secondary growth is MOF synthesis using previous seeding step before continuing to the layer growth step. Seeding is done by depositing the same type of MOF nanoparticles by dip coating, rubbing, spin coating, etc.[16] Other synthesis have also been developed, e.g. layer-by-layer growth, and repeated growth.[17]

MOF thin films and membranes have been utilized widely in the application of selective gas adsorption and gas separation for their properties in size exclusion and adsorbate-MOF surface interaction based separations.[18] There have been plenty of research on this matter, for example H_2 purification and recovery using MOF layers such as MOF-5, HKUST-1, ZIF-8, etc. The others are CO_2 separation and capture with ZIF-69 and ZIF-8 membranes, olefin/parafin separation using ZIF-8 membranes, and liquid separations using various types of MOF such as MIL-53, ZIF-8, ZIF-71, ZIF-78, etc.[17]

Another application of MOF thin films is in the field of chemical sensor, especially in sensing vapors and gases in small concentration, such as nitro-containing molecules for explosives (TNT, DNT and DMNB), xylene, etc. The means of signal transduction of MOF sensors can be varied from electromechanical transduction (micro cantilever, quartz micro balance, surface acoustic wave devices), to luminescence transduction for MOFs that have luminescence effect under the adsorption of certain molecules (e.g. Zn_3btc_2 film for sensing TNT).[12]

1.3 Zeolitic-Imidazolate Framework

Zeolitic-Imidazolate Framework (ZIF) is a subclass of MOF which has a crystalline structure consisting of Zn or Co metal nodes in the form of tetrahedral metal ions and imidazolate organic ligand linkages.[19,20,21] The term zeolitic refers to ZIFs similiarity to zeolite structure, due to the same bond angle of (M – Im – M) in ZIF and (Si – O – Si) in zeolites which is 145^o.[20] There are different types of ZIFs varied by different metal nodes and functional group of imidazolate ligands, some of them have been extensively investigated in scientific journals and listed in Table 1.

Comparing to other subclasses of MOFs, ZIFs hold higher chemical and thermal stability, making it useful for broad applications, such as gas separations, pervaporation and functional devices for ZIFs in the form of thin films.[20]

Table 1 Various types of ZIFs [20]

ZIF type	Molecular structure	Topology	Pore size (nm)	Ref
ZIF-7	Zn(benzimidazole)2	SOD	0.3	21, 22
ZIF-8	Zn(2-methylimidazole)2	SOD	0.34	23, 24
ZIF-9	Co(benzilimidazole)2	SOD	<0.30	23
ZIF-22	Zn(5-azabenzimidazolate)2	LTA	0.3	25
ZIF-69	Zn(5-chlorobenzimidazole)(2-nitroimidazole)	GME	0.44	26
ZIF-71	Zn(4,5-dichloroimidazole)2	RHO	0.42	27
ZIF-78	Zn(5-nitrobenzimidazole)(2-nitroimidazole)	GME	0.38	28
ZIF-90	Zn(imidazolate-2-carboxaldehyde)2	SOD	0.35	29
ZIF-95	Zn(5-chlorobenzimidazole)2	POZ	0.37	30
SIM-1	Zn(4-methyl-5-imidazolecarboxaldehyde)2	SOD	<0.34	31
ZIF-9-67	Co(benzimidazole)(2-methylimidazole)	SOD	<0.34	32

In Figure 4(a), it is shown the crystallographic structure of ZIF-8, as a part of ZIF subclass, which is specifically containing tetrahedral corners ($Zn(mIm)_4$ units) with each Zn^{2+} ions linked with two $(mIm)^-$ ligands to form a 3D sodalite (SOD) structure with a pore size of 3.4 Å.[21] The SOD structure is similiar to the topology of Zeolite A and will form tiling, shown in Figure 4(b).

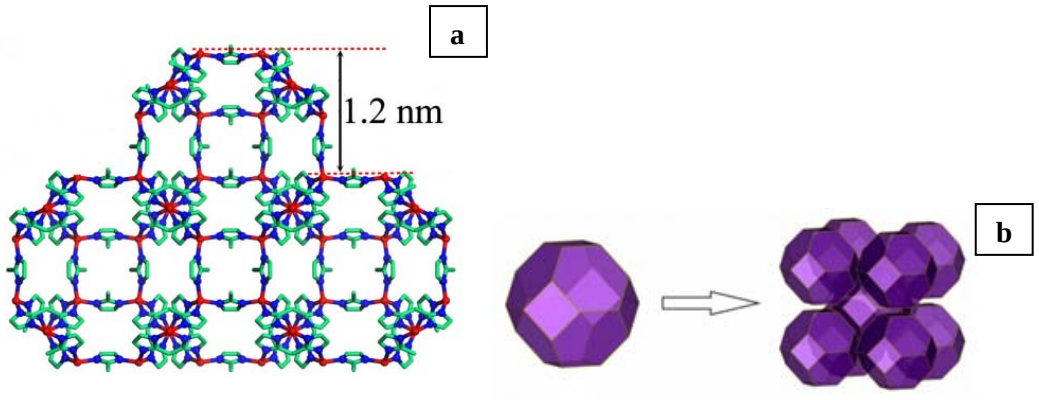

Figure 4 (a) ZIF-8 structure viewed along the [100] direction with the crystallographic spacing d110 of 1.20 nm. Red: Zn; Blue: Nitrogen atom; Green: mIm cyclic molecule; H atoms have been omitted for clarity.[21]; (b) ZIF-8 SOD structure tiling [33]

ZIF-8 thin film is synthesized based on direct synthesis and secondary growth method, as well as other methods summarized in Table 2, 3 and 4. The direct synthesis method is straight forward and does not include many different steps. Nevertheless, the resulted thin films often have intercrystal voids which are unfavorable in some applications, especially in gas separation membrane fabrication.[20] On the other hand, the secondary growth have been known to be more effective in thickness and crystal orientation control.[20] The drawbacks of secondary growth is more synthesis steps of ZIF-8 seed crystal which is done by solvothermal methods such as the one produced by Park et al.[34]

ZIF-8 layers have been showing good performance in the application of H_2 separation and recovery due to ZIF-8 small pore size, so that it is able to act as molecular sieve for the selectivity of H_2 molecules (kinetic diameter of 2.9 Å) from other bigger molecules.[17] ZIF-8 is also known to exclude selectively water molecules for its hydrophobic properties.[23] Other applications such as, hydrocarbon separation and chemical vapors detection have also been tested by researchers shown in Table 3 and 4.

Table 2 ZIF-8 syntheses by direct synthesis method

Substrate	Solvent	Synthesis temperature (^oC)	Heating media	Film thickness (µm)	Synthesis time (h)	Application	Ref
N/A (ZIF-8 nanoparticles)	DMF	140	Oven	-	4	Hydrogen adsorption	34
Titania	Methanol	100	Microwave oven	30	4	H_2/CH_4 gas separation (H_2 selective)	23
ZnO deposited alumina	Methanol	120	Oven	25	4	N/A	35

The main advantage of using methanol as solvent in the synthesis is that it has smaller kinetic diameter and weaker interaction with ZIF-8 framework compared to DMF. Therefore, methanol removal from the pore network is easier.[23] ZIF-8 precursors are more soluble in methanol in room temperature compared to water. Moreover, methanol has high volatility for the ease of film drying after the synthesis.[20]

Table 3 ZIF-8 syntheses by secondary growth method

Substrate	Solvent	Seeding method	Synthesis temperature (°C)	Heating media	Film thickness (µm)	Synthesis time (h)	Application	Ref
Alumina	Water	ZIF-8 particles seeding	30	Oven	2.5	6	C_2/C_3 hydrocarbon gas mixtures separation (ethane/propane, ethylene/propylene and ethylene/propane)	36
Alumina hollow fiber	Water	ZIF-8 particles seeding	25 - 100	Oven	1.4	6 - 72	Single membrane permeation test of H_2, N_2	37
Alumina tube	Methanol	ZIF-8 particles seeding	110	Oven	5	4	H_2/CO_2, H_2/N_2 and H2/CH_4 gas separation	38
Yttria-stabilized zirconia hollow fiber	Water	ZIF-8 particles seeding	30	Oven	2	6	Highly H_2 permeable membrane	39
Alumina	Methanol	ZIF-8 particles seeding	25	-	~1	<6	C_3H_6/C_3H_8 and CH_4/n-C_4H_{10} gas separation	40
Polyethersulfone	Methanol	ZIF-8 particles seeding	90	Oven	7.2	6	H_2 separation membrane	41
Carbon nanotube	Methanol	ZIF-8 particles seeding	25	-	5 - 6	3 - 6	Gas separation enhancer of the vertically-aligned carbon nanotubes	42
Anodic aluminium oxide membrane	Methanol	Fast *in situ* seeding	25	Ultrasound	-	4	Gas separation membrane (H_2/CO_2 and H_2/N_2)	43
APTES functionalized alumina hollow fiber	Water	Cyclic flow (continuous) secondary growth	30	Oven	2	6	H_2 recovery	44
Alumina	Methanol	Hot support seeding	200 (seeding) 120	Oven	12	0.3 36	H_2/CH_4 gas separation (H_2 selective)	45
Alumina hollow fiber	Methanol	Hot support seeding	150 (seeding) 25	Oven -	20	4 0.3	High H_2 permselective membrane	46

Table 4 ZIF-8 syntheses by other methods

Substrate	Solvent	Synthesis method	Synthesis temperature (^oC)	Heating media	Film thickness (μm)	Synthesis time (h)	Application	Ref
Alumina holow fiber	Methanol	Repeated growth	150	Oven	6	5 per cycle	H_2/CO_2, N_2/CO_2 and CH_4/CO_2 gas separation	47
Polyethersulfone	Methanol	Layer-by-layer growth	25	-	10	30	Gas separation membrane (H_2/CO_2 and H_2/C_3H_6)	48
Alumina	Methanol	Precursor infiltration	50	Oven	10	4	H_2 selective membrane	49
Alumina holow fiber	Methanol	ZnO deposition and reactive seeding	100	Oven	8	5	Gas permeation and permselectivity	50
Nylon	Methanol	Counter-diffusion	25	-	16	16 - 72	Gas separation membrane (H_2/N_2)	51
Nylon	Water	Counter-diffusion	25	-	2.5	16 - 48	H_2 selective membrane	52
APTES functionalized alumina tube	Methanol	Counter-diffusion	150	Oven	2	5	H_2 selective membrane	53
Alumina hollow fiber	Methanol	Counter-diffusion	50	Oven	70	12 - 96	Propylene/propane separation	54
Silicon wafer	Methanol	Repeated growth	25	-	<5	0.5 per cycle	Selective sensor for chemical vapors and gases (n-hexane/cyclohexane, ethanol/water)	55
Silicon wafer	N/A (solvent free)	ZnO deposition and thermal synthesis	160	Oven	1 - 5	0.3	N/A	56

Ceramic membranes, e.g. alumina and titania have been utilized in ultrafiltration application[57] and incorporation of ZIF-8 layers are intended to improve the material selectivity towards certain gases, especially H_2. The ceramic hollow fiber and tube shaped supports, have the advantage of easy assembly into compact modules which is applicable directly in industrial separation processes.[20] Polymeric supports are favorable due to the good compatibility between ZIF-8 and polymeric compounds taking into account the interaction between the polymers and the organic ligands.[20] Silicon wafer is an option for ZIF-8 thin film support for the application in microdevices, in regards to the ability to produce microdevices using integrated zeolite films on silicon wafers[3,4,6,7,10], and the synthesis method obtained by Lu et al.[55]

Other synthesis methods shown in Table 4, were conducted to improve direct and seeded growth syntheses. For the application in microsensors, Lu et al.[55] have conducted a method of synthesis in room temperature for the compatibility to the working condition in the clean room. Stassen et al.[56] have also improved Lu et al. methods by a solvent-free synthesis. Nevertheless, higher reaction temperature is needed for this method. Counter-diffusion method, in which the two precursor solutions are separated by porous supports, can be used to grow intergrown layer without the complexity of secondary growth processes.[58]

1.4 Metal-Organic Framework patterning

For the objective of higher surface-to-volume ratio of MOF layers, which will lead to higher adsorption accessibility of gases, layer patterning is needed.[59] Several experiments have been conducted to achieve controlled patterns of MOF deposition. The growth of MOF-5, for example was successfuly controlled by previously functionalizing the support with Self-Assembly Monolayer (SAM) which has carboxylic acid functional groups that bond better with MOF-5 precursors. SAM was obtained by soft lithographic micro contact printing (μCP) or electron beam lithography (EBL).[16] Other functionalization is selective seeding of the support with ZIF-7 crystals to controlly grow ZIF-7 pattern.[60]

Another method of patterning involve external control of the growth of MOF. Electrochemical induced synthesis was done by Ameloot et al.[61] for patterned deposition of HKUST-1 on copper substrates. Controlled deposition of HKUST-1 solution drops on patterned wells was also conducted by using dip-pen nanolithography.[62]

Patterning can also be done after the growth of the MOF layer, for example the patterning of ZIF-8 layer by photolithography done by Lu et al.[63] and ZIF-9 layer using X-Ray lithography by Dimitrakakis et al.[64]

2. Objectives

This Final Master Project consists of studies of Metal-Organic Framework layer. ZIF-8 layer has been chosen, taking into account of its thermal stability and its applications in hydrogen purification and gas sensor, also considering its ease of synthesis which can be conducted in room temperature, using methanolic precursor solutions; a method that could be directly implemented in clean room processes.

The goal of this Final Master Project is to integrate ZIF-8 layer in various microdevices (mainly microsensor, micro preconcentrator and self-standing micro membrane) and a composite membrane. The challenge is to utilize the already developed methods in the literature for the synthesis of ZIF-8 together with the experiences of patterning zeolites developed in Nanostructured Films and Particles Group (NFP) of Instituto de Nanociencia de Aragon (INA) to reach the goal. The specific goals are described in Figure 5 and consist of:

- *ZIF-8 layer on silicon based supports;*
  A. ZIF-8 microsensor
  B. ZIF-8 micro preconcentrator
  C. ZIF-8 free-standing micro membrane
- *ZIF-8 layer on polymer based supports;*
  D. ZIF-8 free-standing micro membrane
  E. PBI/ZIF-8 composite membrane

In order to reach the goals, the work is divided into the following tasks;

a. Synthesis of ZIF-8 layer on silicon support
   - ZIF-8 layer growth
   - Chemical stability tests of ZIF-8 layer (etching and ultrasound treatments of the layer)
   - Patterning ZIF-8 layer by UV lithography

b. Synthesis of ZIF-8 layer on patterned silicon support
   - Patterning silicon support by UV lithography
   - ZIF-8 layer growth on the patterned support

- Packaging the layer and building the micro preconcentrator device

c. Synthesis of defect-free ZIF-8 layer on Si_3N_4 and SiO_2 grid supports
   - ZIF-8 layer growth on the grid supports
   - Back-etching silicon layer and formation of free-standing ZIF-8 membrane

d. Synthesis of defect-free ZIF-8 layer on SU-8 support
   - ZIF-8 layer growth on the patterned SU-8 support
   - Back-etching the support and formation of free-standing ZIF-8 membrane

e. Synthesis of PBI/ZIF-8 composite membrane

Figure 5 Schematic goals of the Final Master Project in ZIF-8 layer integration in microdevices and membrane

3. Experimental

3.1 Materials

Precursors of ZIF-8 layer synthesis, zinc nitrate hexahydrate ($Zn(NO_3)_2.6H_2O$) and 2-methylimidazole (mIm), and anhydrous methanol 99.8% (MeOH) was purchased from Sigma-Aldrich.

The UV Lithography process used commercial adhesion promoter (TI Prime) and reversible photoresist (TI 35 ES) obtained from Microchemicals. The photo developer was purchased from AZ Electronic Materials and acetone from Panreac.

Etching solutions consisted of tetramethyl-ammonium hydroxide 25% (TMAOH) was obtained from Fluka-Analytical, and potassium hydroxide 45% (KOH) and nitric acid 64 - 66% (HNO_3) were from Sigma-Aldrich.

3.2 ZIF-8 layers on silicon based substrates

Based on the objectives of integrating ZIF-8 layers in microdevices, silicon substrates were chosen, taking into account of the previous experiments by Lu et al.[55], the well establishment of silicon manufacturing technology in the semiconductor industry and the availability of developed micromachining methods of silicon substrates in Instituto de Nanociencia de Aragon (INA).

3.2.1 ZIF-8 layer synthesis on silicon substrate

The syntheses of ZIF-8 layers were done by following the synthesis method established by Lu et al.[55], begun with small scale growth to obtain a reproducible results and continued with up-scaling synthesis on 3” silicon wafers. Silicon wafers (p-type and double polished with the crystal orientation of 100) were obtained from INA.

Small scale growth

Small pieces of silicon wafer (2 x 2 cm^2) were used as substrates for ZIF-8 layer growth. Substrates were cleaned in a piranha solution, with the composition of 70:30 (v/v) H_2SO_4/H_2O_2, at 70^oC for 30 minutes in order to get the surface of the silicon free off organic substances. Rinsing was done using distilled water and drying with nitrogen flow.[55]

Methanolic solutions of $Zn(NO_3)_2.6H_2O$ (25 mM) and mIm (50 mM) were prepared. Previously cleaned silicon substrates were put on Teflon holders and immersed in fresh mixture that consisted of 10 mL of the $Zn(NO_3)_2$ solution and 10 mL of the mIm for 30 minutes at room temperature (see experimental set-up in Figure 6). ZIF-8 deposited substrates were then washed by immersion in methanol and dried with nitrogen flow. To obtain thicker layers, the process was repeated. In order to investigate the effect of number of cycles on layer thickness, different number of cycles (10, 15, and 20 cycles) were done.[55]

Figure 6 Experimental Set-up of ZIF-8 layer growth on silicon wafer pieces

Up-scale growth

In order to obtain homogenous ZIF-8 layer on 3-inch silicon wafers, three different holder materials had been selected: Polyamide (PA), Teflon (PTFE) and glass (shown in Figure 7), taking into account the possibilities of machining the two polymeric materials and the already tested inert glass containers in the small scale synthesis.

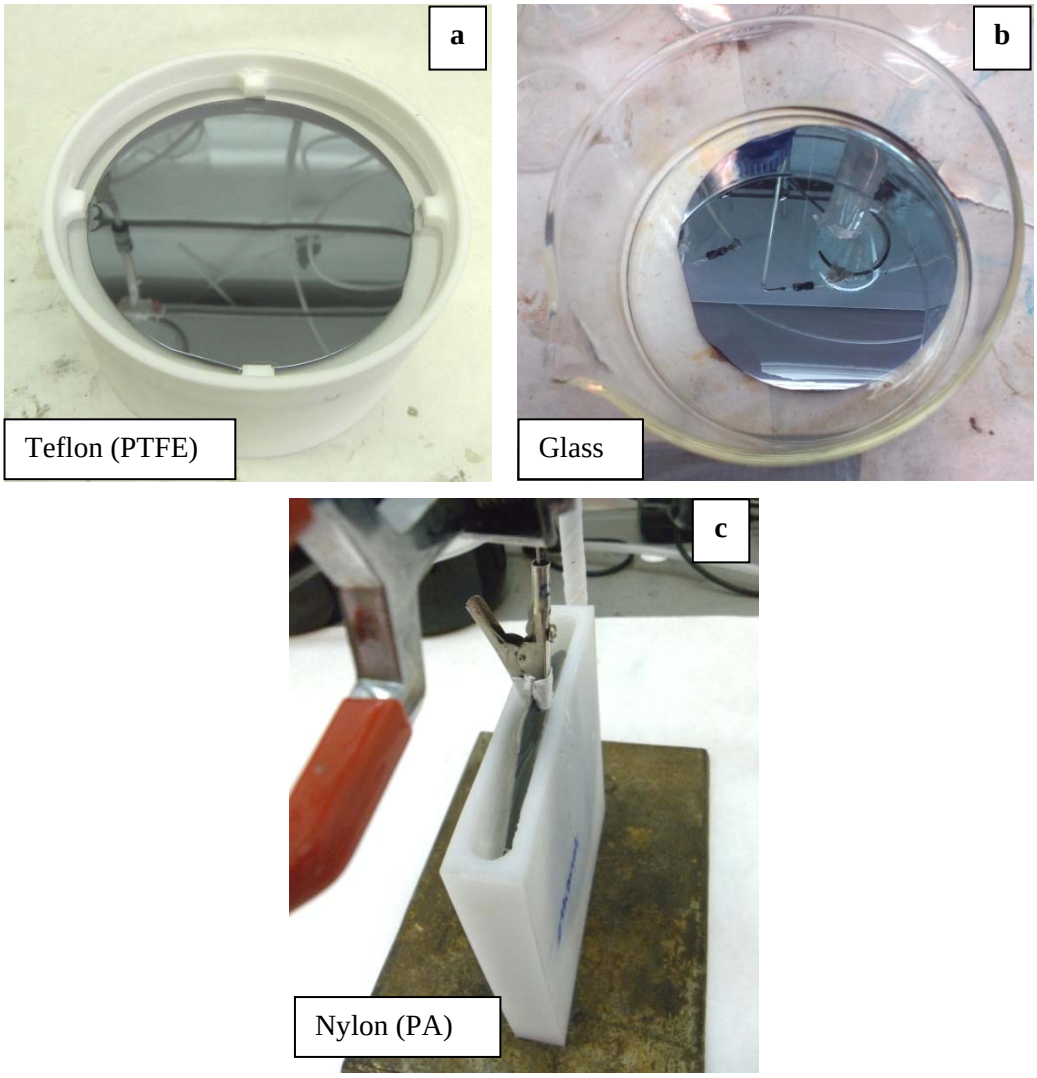

Figure 7 Silicon wafer containers. (a) PTFE, (b) glass and (c) PA holders

3.2.2 ZIF-8 layer synthesis on Si_3N_4 and SiO_2 substrates

Si_3N_4 and SiO_2, with or without grids, were produced in Mesa Institute of Nanotechnology of the University of Twente in The Netherlands, by deposition of thin layers of SiO_2 and Si_3N_4 on silicon wafers. Grid supports were obtained by patterned deposition using UV lithography method. Both supports are represented in Figure 8 and 9. ZIF-8 layer was grown on Si_3N_4 and SiO_2 substrates using the same immersion method described in Section 3.2.1 and were conducted until 20 cycles of synthesis.

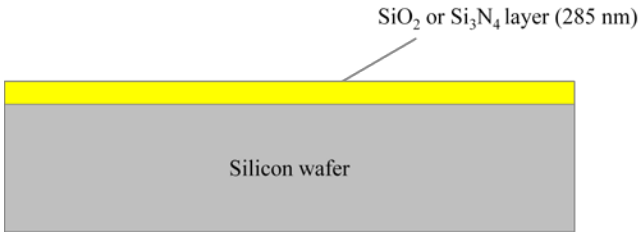

Figure 8 Schematic cross section of SiO_2 or Si_3N_4 support (without grids)

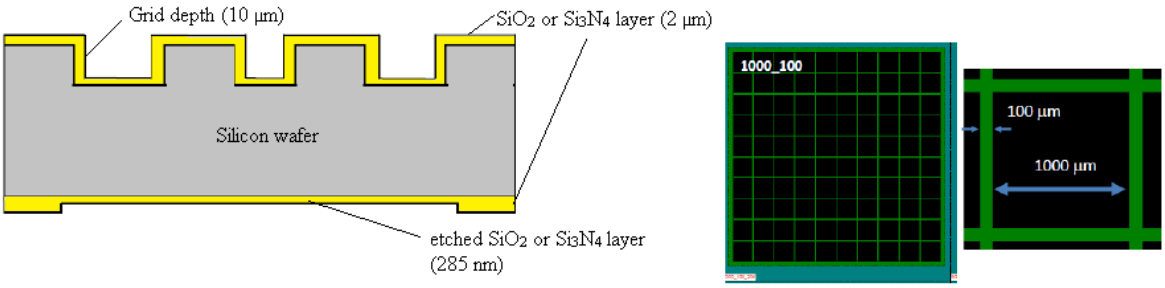

Figure 9 Schematic cross section and top view of SiO_2 or Si_3N_4 support (with grids)

3.2.3 Patterning of ZIF-8 layer

ZIF-8 thin film could be integrated into the application of gas sensor by patterning the synthesized layer.[63] The patterning method that was chosen for this work was UV

Lithography, based on the effective result tested by Lu et al.[63] and the established method of UV lithography which was available in INA.

Chemical stability tests of ZIF-8 layer

In order to have controlled patterning of the as-synthesized ZIF-8 layers, preliminary tests (effect of chemical etching, ultra sounds and acetone to the stability of the layers) were conducted. The tests were done by treating the as-synthesized ZIF-8 layers on silicon supports by various ways described in Table 5.

Wet reaction treatments were conducted by immersion of samples in the reactive solution of different reaction time (see Table 5). The reactive ion etching process (RIE) was done in SISTEC – RIE 600 apparatus with RIE parameters of; oxygen flux = 150 sccm, plasma pressure (Pf) = 0.19 mbar, radio frequency power (RF) = 200 watts and bias voltage = 5 V. The RIE process was conducted in the Clean Room Class 1000 in INA.

Table 5 Chemical stability test of ZIF-8 layer

Reactives	Reaction Time
MeOH + Ultra Sound	2 min 5 min 15 min
Acetone	2 min
Acetone + Ultra Sound	1 min 2 min
KOH	5 s
TMAOH	5 s
diluted HNO_3	5 s 10 s 15 s 20 s
RIE O_2	1 min 3 min 5 min

ZIF-8 layer patterning by UV lithography

In regards to the results that was obtained from the chemical stability tests of ZIF-8 layers, the patterning of as-synthesized ZIF-8 layers on silicon wafer was done by incorporation of O_2 plasma RIE in the Clean Room Class 100 and 1000 in INA. The procedure followed the protocol represented in Figure 10. Process parameters of the lithography procedure are shown in Table 6.

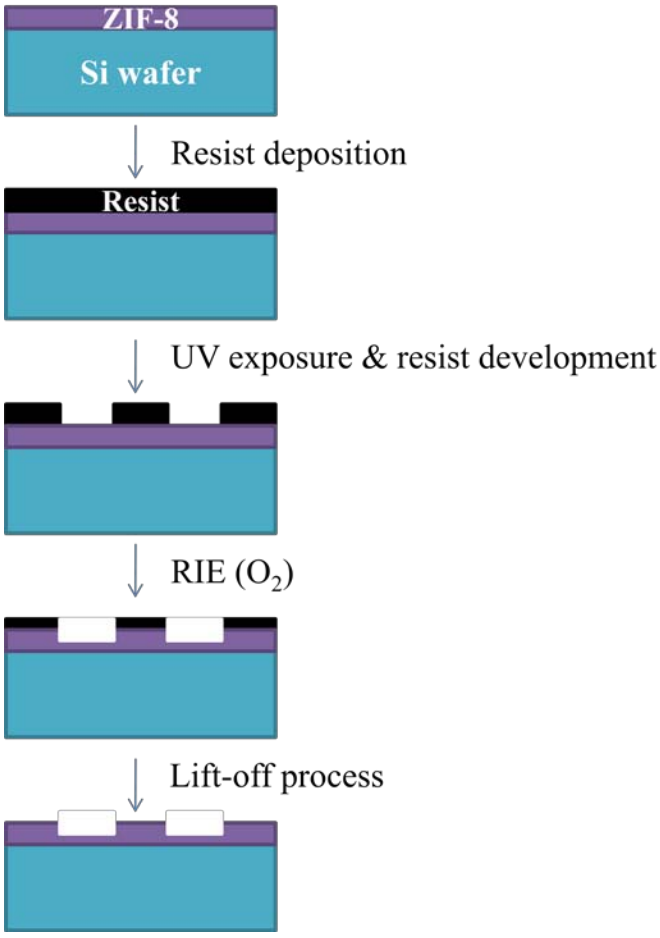

Figure 10 Schematic representation of UV lithography test of ZIF-8 layer

Table 6 ZIF-8 layer patterning protocol

Step	Process	Process Parameters		Equipment
1.	**ZIF-8 Layer Synthesis**	20 cycles		-
2.	**UV Lithography**	Substrate Heating	T = 120 ºC; t = 10 min	SUSS MicroTec Delta 20T2
		Adhesive deposition	Spin coating 4000 rpm	
		Adhesive activation	T = 120 ºC; t= 2 min	
		Positive resist deposition	Spin coating 4000 rpm	
		Soft bake	T = 100º C ; t = 2 min	
		UV exposition	Hard contact t = 25 sec Mask = oxygenator	SUSS MicroTec MA6/BA6
		Waiting time	1 min	-
		Pattern revealing	Diluted AZ Developer : H_2O = 1:1 t = ± 50 s	-
		Inspection under optical microscope	-	ZEISS
		Hard bake	T = 140º C; t = 2 min	SUSS MicroTec Delta 20T2
3.	**Reactive Ion Etching (RIE)**	Reactive = O_2 Pf = 0.19 mbar RF = 200 watts Bias = 5 V Gas flux = 150 sccm t = 10 min		SISTEC – RIE 600
4.	**Lift-Off Process**	Method = rinsing using acetone		-

3.2.4 ZIF-8 layer synthesis on patterned Si substrate

Substrate patterning and ZIF-8 layer synthesis

For the purpose of integrating ZIF-8 layers in the fabricaton of micro preconcentrator, ZIF-8 layer was synthesized on patterned channels of the silicon support. The UV lithography method of channeling silicon wafers was the same of the one to pattern ZIF-8 layer, with differences in the order of the protocol and some parameters of the RIE process. The steps and process parameters of this experiment is shown in the scheme in Figure 11 and in Table 7.

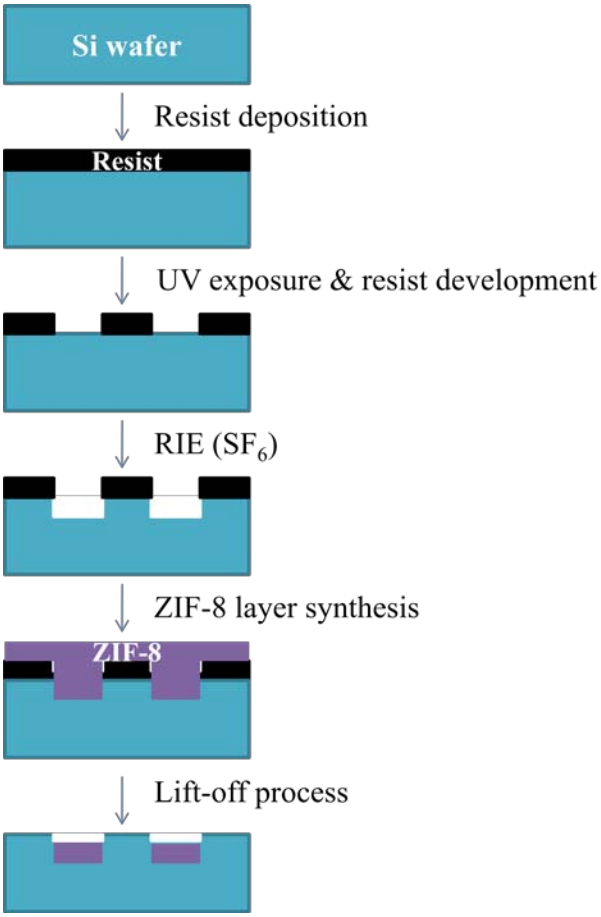

Figure 11 Schematic representation of UV lithography steps in patterning silicon wafer, continued by ZIF-8 layer growth on the patterned support

Table 7 Patterning silicon wafer and ZIF-8 layer growth protocol

Step	Process	Process Parameters		Equipment
1.	**UV Lithography**	Substrate Heating	T = 120 ºC; t = 10 min	SUSS MicroTec Delta 20T2
		Adhesive deposition	Spin coating 4000 rpm	
		Adhesive activation	T = 120 ºC; t= 2 min	
		Positive resist deposition	Spin coating 4000 rpm	
		Soft bake	T = 100º C ; t = 2 min	
		UV exposition	Hard contact t = 25 sec Mask = oxygenator	SUSS MicroTec MA6/BA6
		Waiting time	1 min	-
		Pattern revealing	Diluted AZ Developer : H_2O = 1:1 t = ± 50 s	-
		Inspection under optical microscope	-	ZEISS
		Hard bake	T = 140º C; t = 2 min	SUSS MicroTec Delta 20T2
2.	**Reactive Ion Etching (RIE)**	Reactive = SF_6 Pf = 0.19 mbar RF = 200 watts Bias = 5 V Gas flux = 200 sccm t = 30 min		SISTEC – RIE 600
3.	**ZIF-8 Layer Synthesis**	20 cycles		-
4.	**Lift-Off Process**	Method = mechanical scratch of resist layer and rinsing with acetone		-

Micro preconcentrator device packaging and test

Device was closed by anodic bonding of silicon wafer with Pyrex glass which was available in the Clean Room Class 1000. The process was done in a homemade apparatus mounted by Servicio de Apoyo de Investigacion de Universidad de Zaragoza (SAI). The device closure was done by heating the silicon substrate at 300 ^{o}C and putting the Pyrex glass wafer on top of the silicon wafer and applying electrical voltage of 1000 volts.

The closed device was then connected to pipes by first of all making a hole on the glass, at the inlet and outlet of the channel patterns, by sand blaster (alumina sand with the size of 125µm).

3.3 ZIF-8 layers on polymeric substrates

ZIFs are known to have good compatibility with polymeric substances due to the organic content of the framework. Therefore, for the objective of fabricating intergrown, defect-free micro membranes, synthesis of ZIF-8 layers on polymeric substrates were experimented.

3.3.1 Growth of ZIF-8 layers on SU-8 substrates

SU-8 is a type of polymeric materials which have high thermal stability (±300 ^{o}C).[65] Based on this property, the affinity of ZIF-8 crystals to polymeric materials and also the availability of patterned SU-8 supports in INA, the synthesize of ZIF-8 layer on this polymeric support was tested for the objectives of micro membrane fabrication.

SU-8 support was made in Nanostructured Films and Particles (NFP) Group in INA by template molding method. ZIF-8 layer synthesis was done by following the method described in Section 3.2.1 for 20 cycles of synthesis.

3.3.2 Growth of ZIF-8 layers on porous polybenzimidazole (PBI) membranes

PBI/ZIF-8 mixed matrix membranes (MMMs) have been investigated by Yang et al. [66] for the application of high temperature hydrogen purification in the petroleum and chemical industries, taking into account the high thermal stability of both materials individually and the compatibility between the organic ligand of ZIF-8 (2-methyl imidazole) and PBI. Nevertheless, MMMs are known to have drawbacks in poor filler-polymer interaction, filler sedimentation and agglomeration[67]. Research in growing the ZIF-8 layer on the polymeric support has been done to improve the composite membrane properties.

Growth of ZIF-8 layer on porous asymmetric polysulfone was investigated by Cacho-Bailo et al.[67] by repeated solvothermal synthesis method. A thick ZIF-8 intergrown layer (± 35 µm) deposition on the support was obtained and achieved high H_2 selectivity among reported polymer-supported ZIF-8 membranes.

Both Cacho-Bailo et al. and Yang et al. synthesized the composite membrane by incorporation of solvothermal-based ZIF-8 synthesis. In this experiment, a novel method of ZIF-8 layer synthesis on PBI was conducted, following the synthesis method done by Lu et al.[55] that was done in room temperature.

Both porous PBI membranes (see Figure 12) were produced in NFP group in INA. The non-woven electrospunned PBI membranes were obtained by electrospinning method and have average thickness of 45 µm. The assymetric porous PBI membranes were produced by phase separation method of the homogenous polymer solution into a polymer rich and polymer lean phase and have average pore size of 100 nm and thickness of 60 µm.

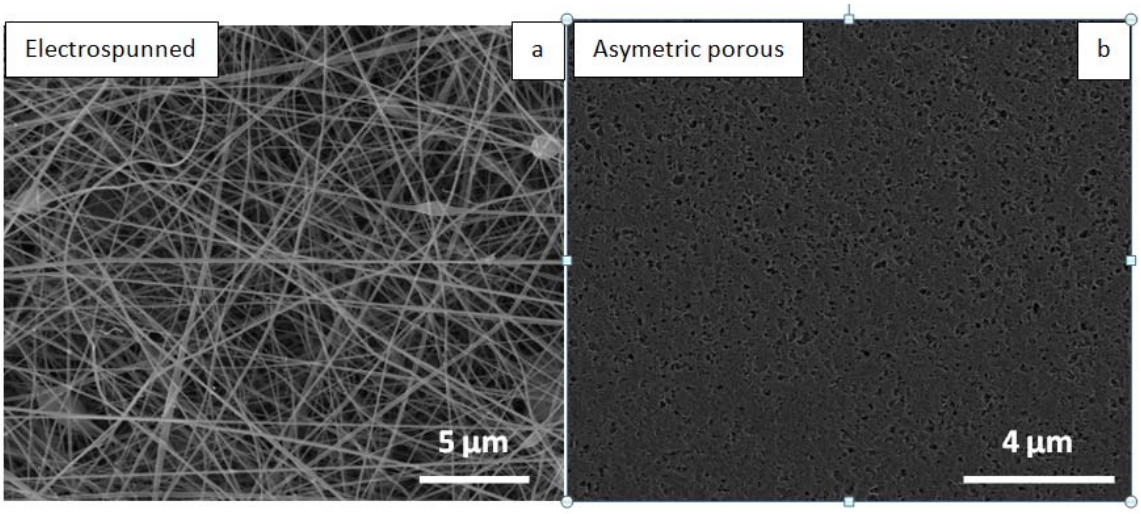

Figure 12 (a) Electrospunned PBI membrane and (b) asymetric porous PBI membrane

The growth was done by the method explained in Section 3.2.1 without Teflon holder and varied for 10, 15, and 20 cycles of synthesis. The synthesis set-ups are shown in Figure 13. The up-scale growth was done using an O-ring stretcher frame from a material of Polyamide (PA) to keep the membrane straight during the synthesis.

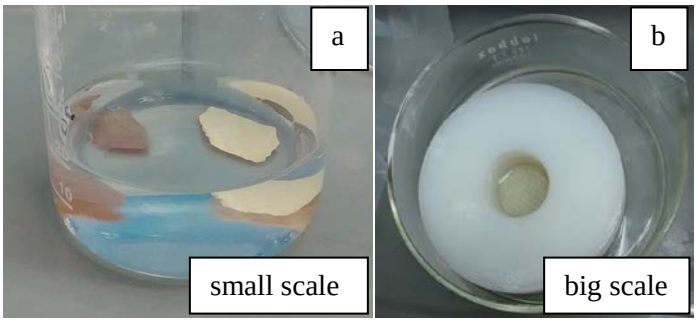

Figure 13 Experimental set-up of ZIF-8 layer synthesis on PBI supports. (a) small-scale trials and (b) big-scale synthesis using PA O-ring strecher frame

The resulted composite membrane was then dried in 120 ^{o}C for 2.5 hours for methanol removal from the framework, and placed in the membrane module of the permeation test equipment available in INA.

3.4 Characterization

3.4.1 Scanning Electron Microscopy (SEM)

SEM (FEI Inspect) was used to characterize the surface of the ZIF-8 layer and also the layer thickness by cross-sectional observation. The samples were placed on a stepped holder by carbon tape. Due to the high porosity of MOFs, these materials are known to be beam sensitive and the accelerated electron beam damages them. Therefore, samples were coated by platinum coating which was deposited by sputtering method using EMITECH CA 7620 Sputter Coater with an electric current (I) of 15 mA for 90 seconds. Pt-coated samples were observed in the SEM at low voltage 2 kV and spot size 2.0 to minimize the risk of framework collapsing due to electron beam exposure. In order to make sure about the layer boundaries between the support and the ZIF-8 layer, Energy Dispersive X-Ray Analyzer (EDX: INCA PentaFET X3) attached to the microscope was utilized.

3.4.2 Profilemeter

The Profilemeter (KLA Tencor P-6) was mainly used to check the thickness difference between one part of a sample which was etched (by several etching methods; RIE using SF_6 and O_2 as reactive, wet etching using diluted HNO_3) and the part which was not due to layer coverage using Kapton tape during the etching process.

3.4.3 X-Ray Diffraction (XRD)

XRD was used to check the crystallography of the deposited layers on the silicon substrate, whether it matches the crystallography of ZIF-8 thin films or not. XRD characterization was done in Servicio de Difracción de Rayos X y Análisis por Fluorescencia del Servicio General de Apoyo a la Investigación de la Universidad de Zaragoza.

The datas were obtained at ambient temperature using D-Max Rigaku difractometer equipped by a rotating anode and worked at 40 kV voltages and 80 mA current. Measurement conditions were: $2\theta = 2.5 – 40^{o}$, step = 0.03^{o} and t = 1 s/step.

3.5 Distillation of the methanolic waste solution

Methanolic waste of ZIF-8 layer synthesis and washing was kept to be distillated in order to recover clean methanol. Distillation was done using rotavapor (Heidolph HEI-VAP Advantage) equipped with a spiral tube condenser.

The waste solution was heated in oil bath at 110^{o}C and 50 rpm rotation speed. The process was done without vacuum pump to avoid rapid vaporization and loss of methanol. The methanol vapor was condensed by cooling tap water and accumulated in the rounded glass container. The connections of the apparatuses in the distillation system were closed by Teflon tape instead of vacuum grease, so that there was not any organic contaminant in both waste and distilled methanol. The distillation process was repeated three times to maximize the purification of methanol.

Distilled methanol was then used to synthesize ZIF-8 layers based on the 15 cycle process as explained in section 3.2.1, in order to proof if it can be recycled. Recovery of methanol from the methanolic waste can be successfully conducted by a 3-cycle distillation method. Synthesis of ZIF-8 layer using recycled methanol has less homogenous thickness due to impurities in the distilled methanol container and the laboratory environment.

4. Results and discussion

4.1 ZIF-8 layers on silicon based substrates

The synthesis method proposed by Lu et al.[55] was followed and the reproducibility of the method was obtained by taking into account of details, such as cleaning of silicon supports, utilization of fresh mixture of solution and clean containers.

4.1.1 ZIF-8 layer synthesis on silicon support

Importance of silicon support cleaning

The cleaning step of substrate preparation plays an important role in terms of homogenous growth of the ZIF-8 layer. This is related to the energetic of nucleation stage of crystals to form stable clusters. The energy needed for the system to form stable clusters (with the radius r* in Figure 11) is defined as critical energy barrier (ΔG_T*) in Equation 1. [68]

Equation 1 Total free energy of nucleation process [68]

$$\Delta G_T = -\frac{4}{3}\pi\frac{r^3}{V}\Delta\mu + 4\pi r^2\sigma$$

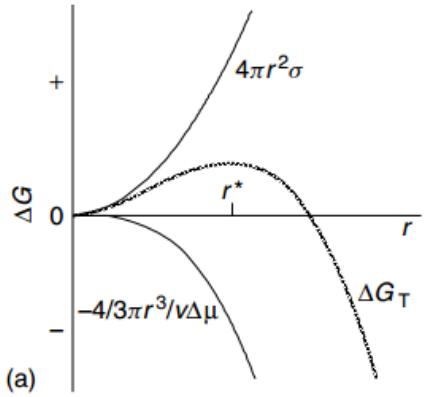

Figure 14 Correlation between total free energy versus the radius of the clusters [68]

ΔG_T is described as the total free energy. The term $(\frac{4}{3}\pi\frac{r^3}{V})$ is defined as the number of molecules contained in each nucleus, assuming spherical shape of the nucleus, $\Delta\mu$ is the difference in chemical potential between a molecule in solution and that in the bulk of the crystal. The term $4\pi r^2$ was the surface area of the spherical nucleus and σ is the surface free energy between the solid-liquid interfaces.

In the case of impurities in the experiments, the presence of organic molecule on the surface of the substrate changes the surface free energy of some parts of the substrate, hence inducing heterogeneous nucleation of ZIF-8 on diverse area across the surface of the support, and formation of crystals with wide distribution of size. Therefore, imperfectly cleaned silicon substrate surface will induce less homogenous layer shown in Figure 12(b).

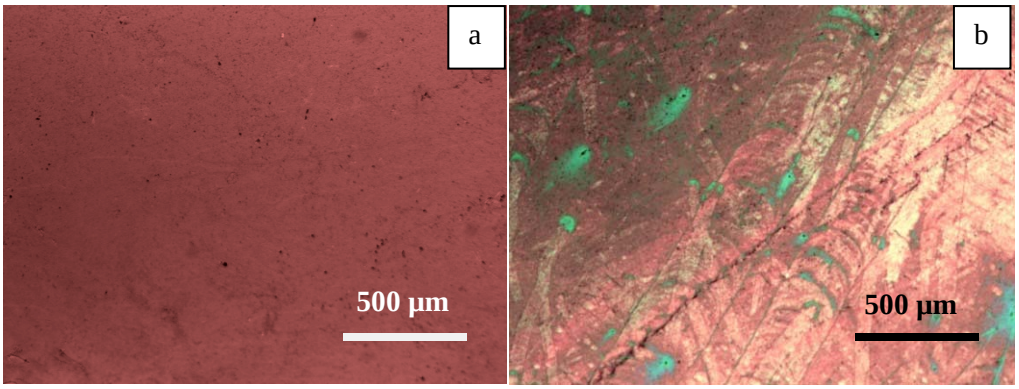

Figure 15 Comparison of 20-cycle ZIF-8 layer syntheses on (a) cleaned and (b) uncleaned silicon substrates

Importance of clean beaker glass

In every cycle of the synthesis, it is also important to use clean glass container instead of the same container as the previous cycles. This is due to heterogenous nucleation of some of the fresh precursors on the ZIF-8 crystals deposited on the glass surface, so that the layer growth on the substrate is not maximized.

Importance of utilization of fresh mixture of precursor solution

Each cycle of ZIF-8 synthesis was done using fresh mixture of precursor solution, so that the layer growth could take place. Based on the experiments of two syntheses of ZIF-8 layers, one using fresh mixture of precursor solution every cycle and the other using the same solution in each cycle, the result of thickness characterization using profilemeter shows that the ZIF-8 layer synthesized using the same solution was not grown as much as the other sample. This is validated by the layer thickness of only 85.5 nm. This thickness profile was in accordance to only one-cycle synthesis.

The number of moles in the precursor solution mixture was calculated and shows that stoichiometrically there are enough $Zn(mIm)_2$ molecules to form 0.41 mm of ZIF-8 layer on a 2 x 2 cm^2 support (calculation described in Apendix 1). Despite the excess amount of precursor molecules, it does not affect the thickness of the layer due to completed crystals formation of the precursors after ± 30 minutes of reaction[56]. Lu et al. [56] used Quartz Crystal Microbalance and exposed the crystal firstly to the $Zn(NO_3)_2$ solution until it reached saturation, then to the mIm solution. The changes in frequency, i.e. mass gain, indicated that after 30 minutes the reaction is completed. The increasing number of cycles, instead, was just increasing the density of the thin film layer according to experiments done by Tian et al.[69]

Small scale growth

ZIF-8 layer growth was conducted for different number of cycles in order to find its effect on layer thickness. Layer thickness was measured by SEM cross-sectional observation, listed in Table 8 and shown in Figure 17. The top-view observation of SEM image shows intergrown layers of ZIF-8 crystals. The

correlation between the number of cycles of synthesis with layer thickness is shown in Figure 16.

Table 8 ZIF-8 layer thickness based on different number of cycles of the synthesis

Sample	Number of cycles	Layer thickness (µm)	
		Per sample	Average
1	10	0.62 ± 0.02	0.63 ± 0.02
2		0.64 ± 0.02	
3	15	1.10 ± 0.02	1.13 ± 0.04
4		1.12 ± 0.02	
5	20	1.47 ± 0.04	1.42 ± 0.07
6		1.37 ± 0.05	

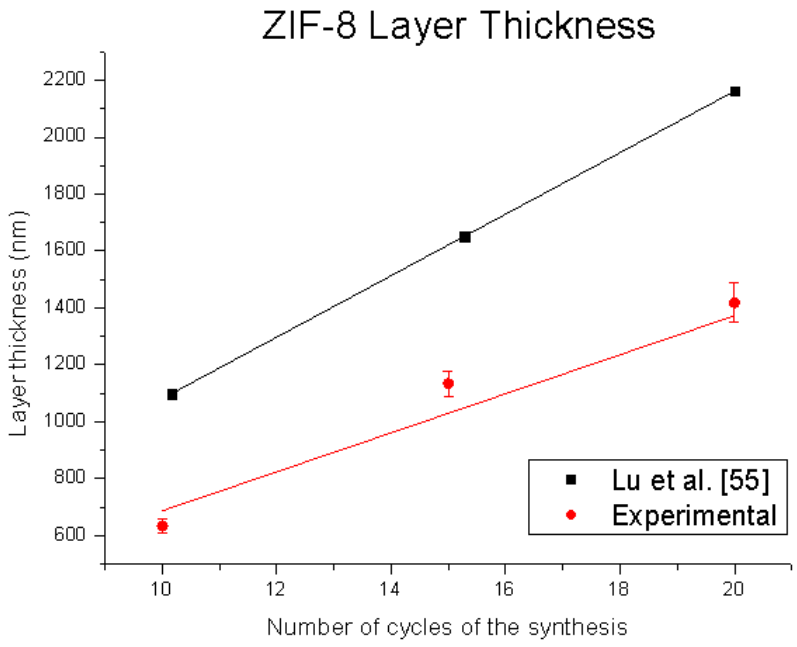

Figure 16 ZIF-8 layer thickness correlation the with number of cycles of synthesis (Lu et al.[55] and experimental)

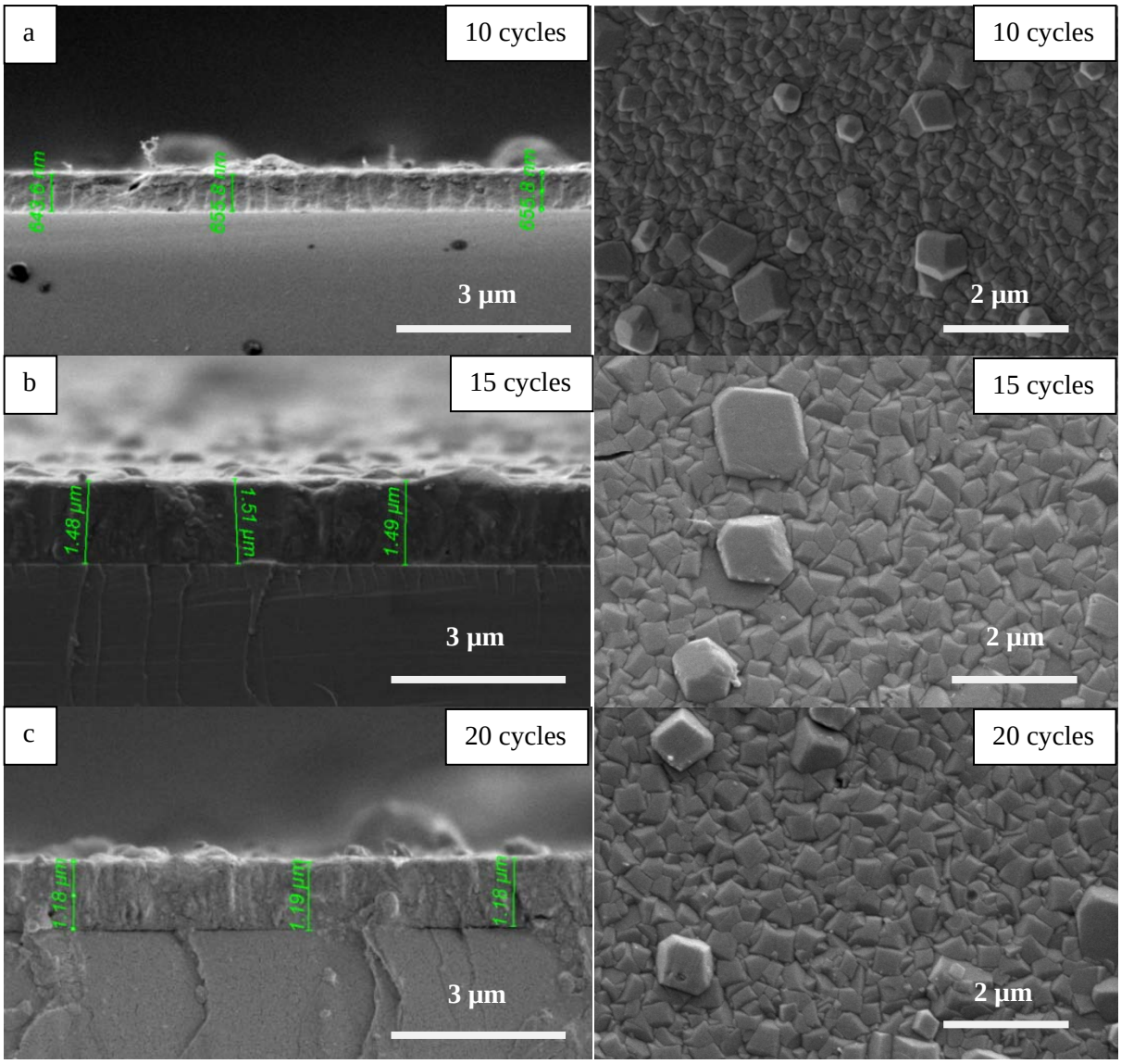

Figure 17 SEM images (cross section – left, top view – right) of ZIF-8 layers for (a) 10-cycle, (b) 15-cycle and (c) 20-cycle syntheses

The correlation between the thickness of the layer and the number of cycles of the synthesis shows a linear function, as can be seen in Figure 16. The average layer thickness which can be obtained each cycle of synthesis is 68.6 nm Compared to the results obtained by Lu et al. [56], the layer obtained is thinner than the one the literature due to possible difference in support holders and

solution containers materials, as well as different surface-to-volume ratio of the synthesis, leading to different path distance of the precursor molecules to the silicon substrate surface.

X-Ray diffraction analysis

The crystallography of a layer sample from 10-cycle synthesis was analyzed by XRD and the peaks are shown in Figure 18.

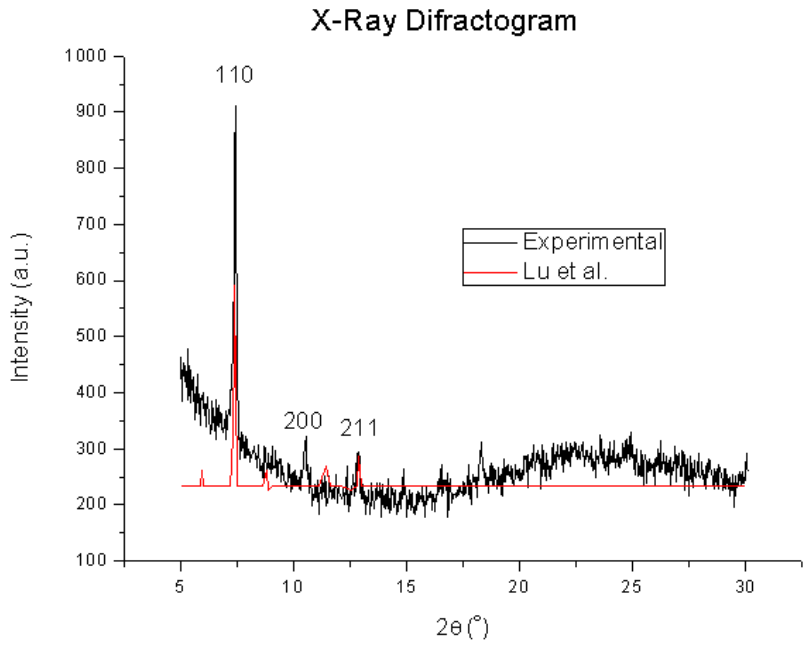

Figure 18 X-Ray difractogram of ZIF-8 layer experimental sample and Lu et al.[55]'s experiments

The X-Ray difractogram of the sample from the experiments are noisy due to the low thickness of ZIF-8 layer compared to the silicon support. The main

crystal orientation preference (110) of the sample matches the ZIF-8 crystallography obtained by Lu et al. This means that the ZIF-8 crystal grow preferably along the direction of (110). The result is in accordance to the report of Cravillon et al.[70] which stated that in room-temperature syntheses, cube-shaped crystals ((100) crystal form) first develop in early stages and eventually transform into rhombic dodecahedra ((110) crystal form). The rhombic dodecahedra shapes and (110) crystal orientation preferences of the ZIF-8 layers obtained in the experiment (shown in SEM top view images in Figure 17) are also in accordance to the shape represented in Figure 19.[71]

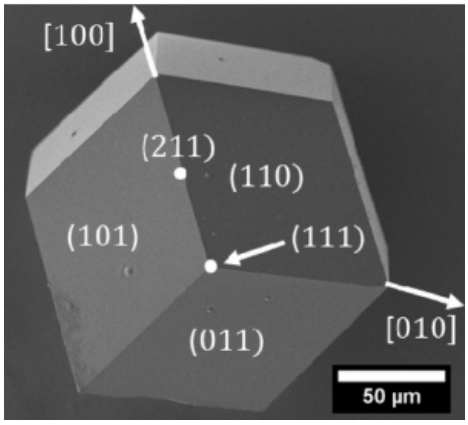

Figure 19 ZIF-8 crystal and its crystallographic orientations [71]

Up-scale growth

Up-scaling was done using three different holders. After 2 cycles of synthesis, the resulted layers of ZIF-8 deposited on silicon wafer contained in polymeric holders shows non-homogeneity, on the other hand the one obtained from synthesis in a glass container had smooth homogenous layer (see Figure 20).

It is also shown that the layer result from the glass container reflects light better than the others.

ZIF-8 crystals have better compatibility with polymers than with the silicon support due to the presence of organic ligands in the framework.[20] Therefore, precursor molecules tend to nucleate more in the polymeric area. Moreover, the surface-to-volume ratios of the polymeric surfaces (1.15 and 2.6 for PTFE and PA respectively) are also higher than the one of the silicon wafer (0.44), without taking into account the roughness of the polymer surface that can increase the ratio. (Calculations shown in Appendix 2)

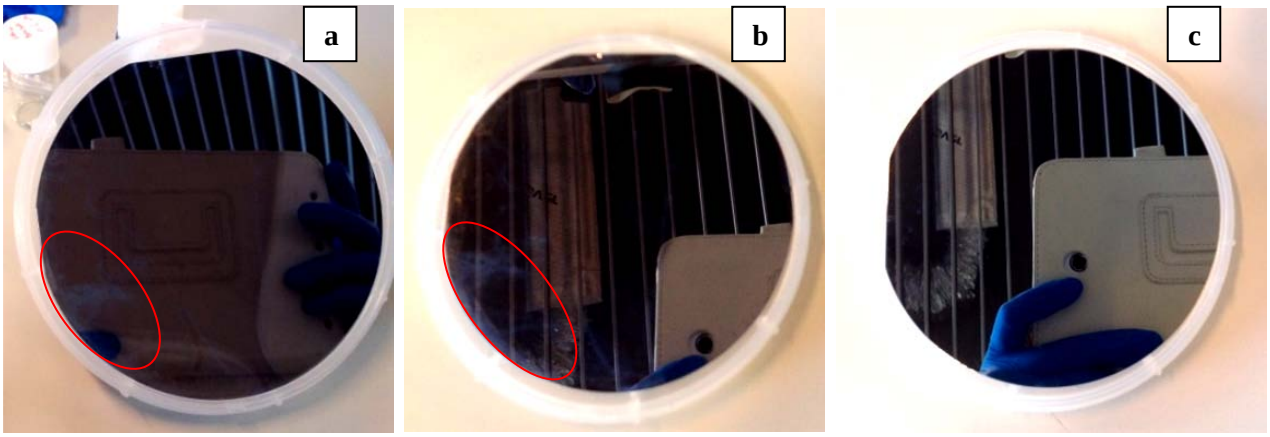

Figure 20 2-cycle synthesis of ZIF-8 layer up-scaled growth in different synthesis containers. (a) Round PTFE, (b) up-right PA and (c) glass containers. Heterogenous depositions are shown in red circles.

4.1.2 ZIF-8 layer synthesis on Si_3N_4 and SiO_2 substrates

Observation of ZIF-8 layer on both Si_3N_4 and SiO_2 supports (in the SEM and optical microscope respectively) shows that the resulted ZIF-8 layers have many cracks

(Figure 21(a)), with the crack-free surface area less than 400 μm^2, compared to the layer on silicon support which is defect-free.

The cracks are hypothesized to be caused by less adhesion of ZIF-8 crystals on the support materials. ZIF-8 material has a hydrophobic nature,[23] so that it has good adhesion to polished silicon substrate (surface energy: 2130 mN/m)[72]. However, it also has good adhesion with polymeric substrates even though they have low surface energy (42.2 mN/m and 19.4 mN/m for PA and PTFE respectively).[73] Si_3N_4 and SiO_2 surfaces, on the other hand, have surface energies of 51.2 and 53.5 mJ/m^2 respectively[74]. From these data, it can be concluded that ZIF-8 crystals adhesion strength is contributed by two factors; mostly by the organic content of the support and also by the surface energy of the support surface.

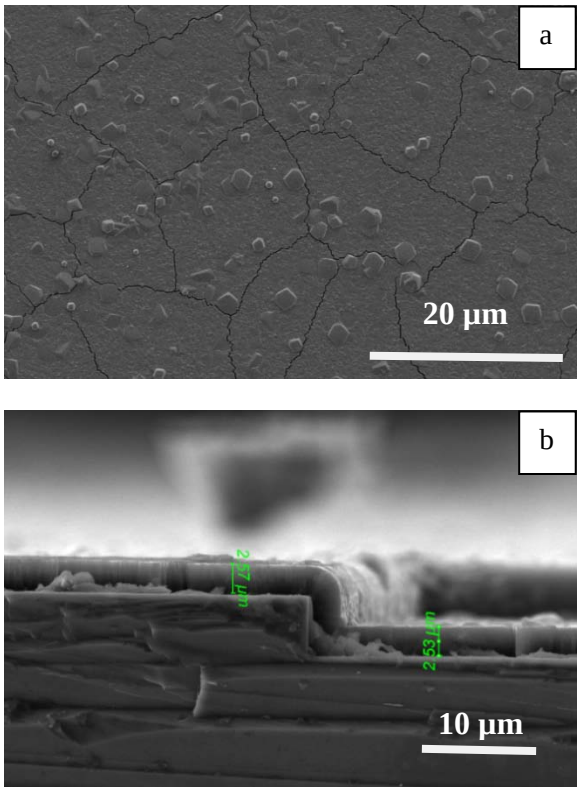

Figure 21 (a) Top-view of ZIF-8 layer on non-grid Si_3N_4 support. (b) Cross-section of ZIF-8 layer on grid Si_3N_4 support

The cracks contribute to membrane defects. Therefore, the layer cannot be integrated in the fabrication of micro membranes, even though that the layer growth was perfectly covering the grid step shown in Figure 26(b), which is one of the good processing factor in producing self-standing membranes.

4.1.3 Patterning of ZIF-8 layer

Experiments were conducted before patterning the ZIF-8 layer to test the chemical stability of the layer towards processes in patterning method, such as etching and lift-off process.

Wet etching of ZIF-8 layer

- *Wet etching using KOH and TMAOH solutions*

Wet etching using KOH and TMAOH solutions were used for the purpose of integrating ZIF-8 layer in the fabrication of free-standing micro membranes on Si_3N_4 and SiO_2 grids. Back-etching of silicon support using basic solutions to build free-standing layer has been widely used. Pellejero et al.[75] fabricated free-standing silicalite cantilever by etching the silicon support using TMAOH solution (25%) at 70 ^oC for 3 hours. Altena et al. [76] used KOH solution for producing free-standing Si_3N_4 membrane.

Stability of ZIF-8 layer was tested in KOH and TMAOH solution. The etching solutions of KOH and TMAOH is considered to be too reactive for ZIF-8 layers because after 5 seconds of sample immersion, all the ZIF-8 layer reacts with the etching reactant and cleaned silicon supports are obtained. This result can lead to loss of ZIF-8 layer during back-etching process of the silicon support.

- *Wet etching using diluted HNO_3 solutions*

Integration of thin films in the fabrication of microsensor has been investigated. Pellejero et al. [75] used HF solution (20 %wt) to pattern silicalite layer as microcantilever sensor.

To etch ZIF-8 layer for microsensor fabrication, Lu et al.[63] used diluted HNO_3. Etching was done to a 200 nm-thick layer, on which some parts were covered by photoresist as a part of UV lithography method. ZIF-8 layer which was exposed to the solution was completely reacted after 5 seconds of etching.

Wet etching test was done using diluted HNO_3 solution (purity 64 – 66%; 1000:1 ratio of H_2O:HNO_3) for ZIF-8 layers produced from a 15-cycle synthesis. The purpose of the experiment is to have a controlled etching method for patterning the ZIF-8 layer. SEM images of etching results are shown in Figure 22. The thickness decreases of wet etching process are listed in Table 9.

Table 9 Wet etching of ZIF-8 layer using HNO_3 solution results

Etching time (seconds)	Layer thickness (µm)	Thickness decrease (µm)
0 (initial layer)	1.42 ± 0.07	-
5	1.05 ± 0.03	0.36
10	0.95 ± 0.02	0.46
15	0.94 ± 0.01	0.47
20	0.95 ± 0.03	0.46

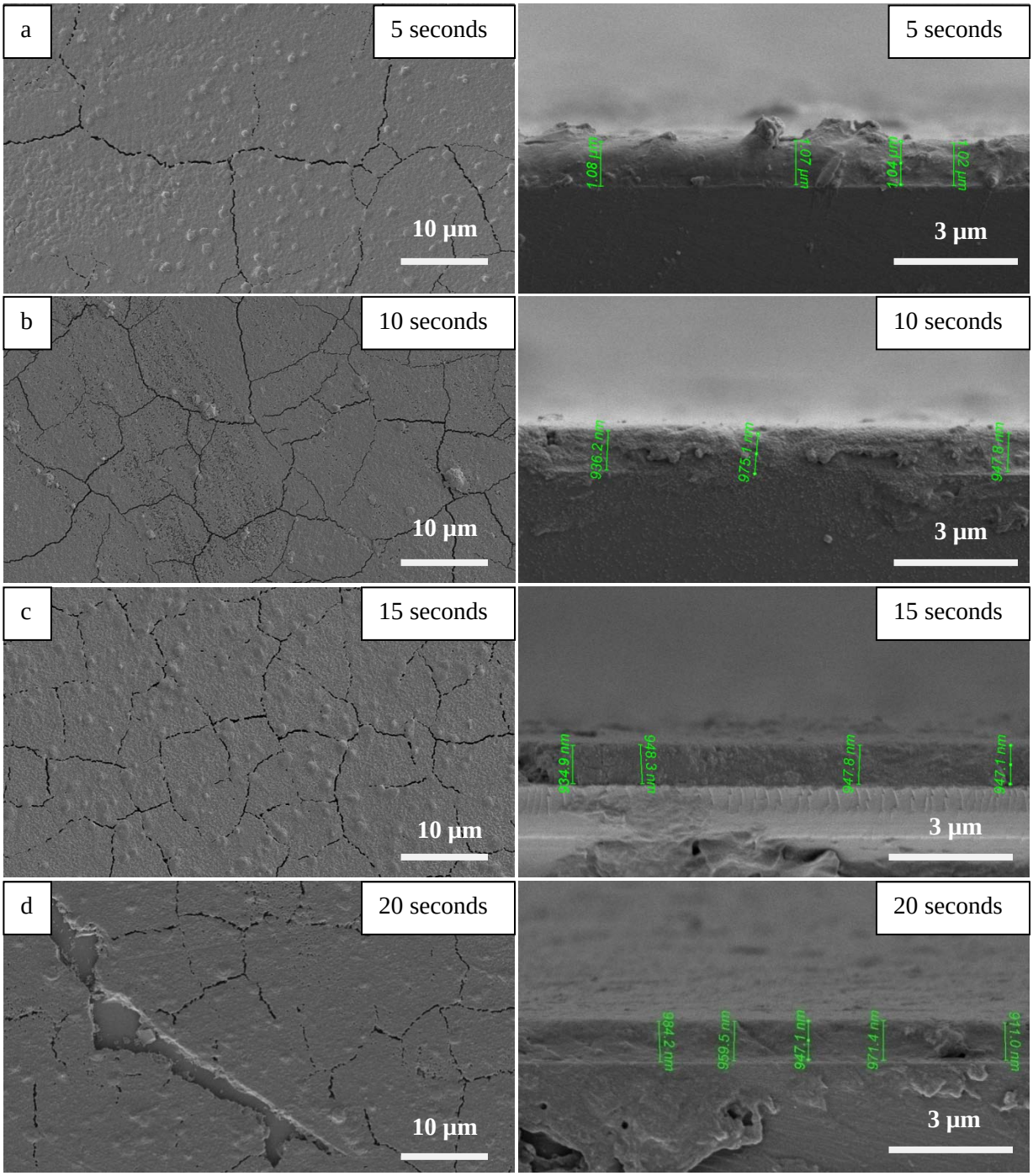

Figure 22 Top-view and cross-section of samples after wet etching using diluted HNO3 solution for (a) 5 seconds, (b) 10 seconds (c) 15 seconds and (d) 20 seconds

The etching results show that it is not possible to establish a controlled etching rate. This is due to ZIF-8 etching mechanism which tends to have individual crystals detachment instead of lateral thickness decrease mechanism. This is in accordance to the tendency of silicalite thin film etched by HF solution that is reported by Pellejero et al.[75]

Lu et al.[63] did not develop experiments to determine the etching rate of ZIF-8 layer. Nevertheless, it is observed that 5 seconds immersion in HNO_3 solution can successfully etch away 200 nm of exposed ZIF-8 layer and make a pattern with pattern side roughness reaching 500 nm. The roughness shown in Figure 19 is possibly due to under etching phenomena and ZIF-8 etching mechanism in acid solution as also observed in the experiments (see Figure 23).

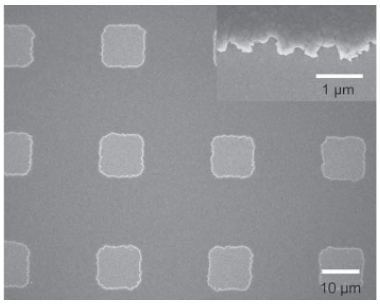

Figure 23 ZIF-8 patterning results obtained by Lu et al.[63], showing pattern edge roughness of 500 nm

Reactive Ion Etching (RIE) of ZIF-8 layer

The experiments were conducted using a 10-cycle synthesized ZIF-8 layer with the layer thickness of 0.63 ± 0.02 µm. The etched layer thickness was measured using profilemeter and thickness decrease was clearly obtained (see Figure 24). However, the etching process produced etched ZIF-8 layer with large rugosity (± 500 nm) as measured using profilemeter and observed using SEM shown in Figure 25.

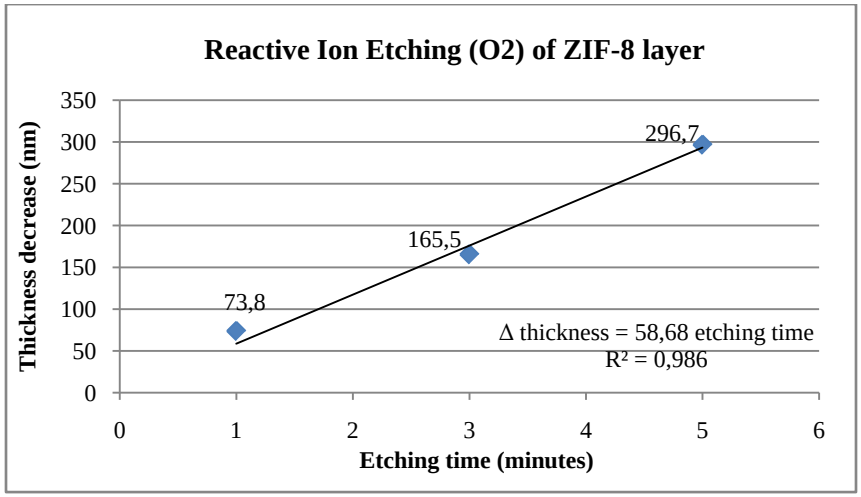

Figure 24 Correlation between etching time and thickness decrease of ZIF-8 layer

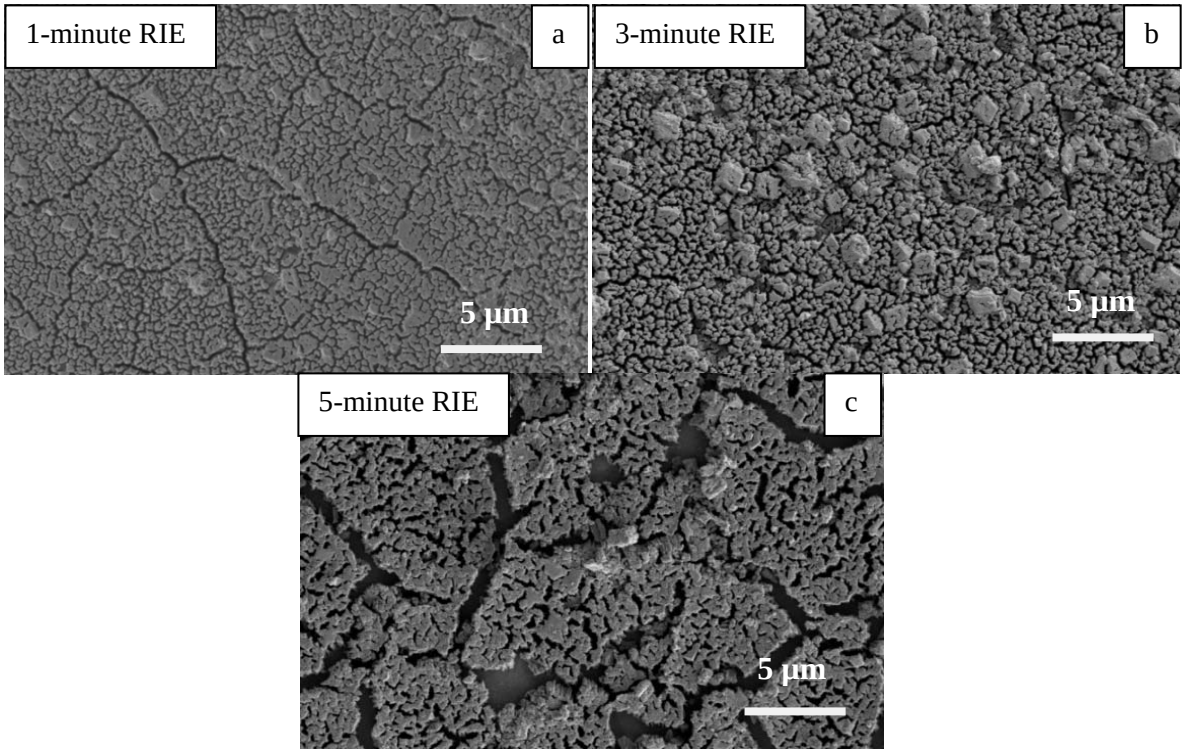

Figure 25 SEM top-view images of etched ZIF-8 layers using RIE method for (a) 1 minute, (b) 3 minutes and (c) 5 minutes

Lu et al.[63] have conducted a novel patterning method for ZIF-8 layer using photo lithography method. In this experiment, a novel method of ZIF-8 layer etching using RIE was tested in order to obtain a method with controlled etching rate. Pellejero et al. [75] used SF_6 as RIE reactant to etch silicalite layer and resulted in under-etching phenomena and rapid etching rate of silicon support.

Reactive ion etching using oxygen plasma has been utilized to etch organic compounds.[77] ZIF-8 layer etching used O_2 plasma RIE to attack the organic ligands in ZIF-8 framework and to avoid etching of silicon parts of the samples which happens in SF_6 plasma.[75]

Based on the results obtained, ZIF-8 layer etching using RIE with O_2 plasma is considered to give more control in thickness decrease by an establishment of an etching rate. Moreover, the distribution of layer holes obtained by RIE is more homogenous compared to the one of the wet etching, especially layer hole shown in Figure 22(d).

Effect of lift-off process on ZIF-8 layers

Lift-off process in UV lithography is the last step in the patterning method to remove the photoresist layer deposition from the substrate. The process is done by dissolution of photoresist layer in acetone. To accelerate the rate of photoresist removal, ultrasound is utilized. Therefore, ZIF-8 layer stability towards ultrasound and acetone were tested.

- *Effect of ultrasound on ZIF-8 layer*

Thompson et al.[78] have conducted experiments about the effect of ultrasound on ZIF-8 nanoparticles. The results show the phenomena of Ostwald ripening of the nanoparticles. Ostwald ripening of ZIF-8 particles happens due to higher temperature in some area (hot spots) that induces ZIF-8 constituents on the surface of the particles to dissolve and be recrystalized on the bigger particles' surface. Therefore, the big particles become bigger and the small ones smaller or even vanished. The prefential growth of bigger crystals happens due to lower thermodynamic stability and surface-to-volume ratio of the smaller particles in the solution.

A sample of a 10-cycle ZIF-8 layer on silicon supports were immersed in methanol and treated for 2, 5, and 15 minutes of ultrasound. The observation in SEM is shown in Figure 26.

The top-view SEM images of the sonicated layers, show changes in the crystal shape compared to the one before sonication shown in Figure 17(a). Some cracks are also observed and even loss of layer after 15 minutes of sonication. Cross section images of the three samples are also represented in Figure 18. The thickness of the ZIF-8 layers after 2 and 5 minutes of sonication was not significantly decreased. The thickness of the layer before sonication was 0.63 ± 0.02 µm. On the other hand, the layer sonicated for 15 minutes had significant layer thickness decrease due to layer detachment as shown in the top-view image.

SEM images show that there are parts which became denser and the other loss the crystals, which explains the cracks, layer detachment and crystal deformation. From these observations, it can be concluded that Ostwald ripening phenomena also appears in ZIF-8 thin layer.

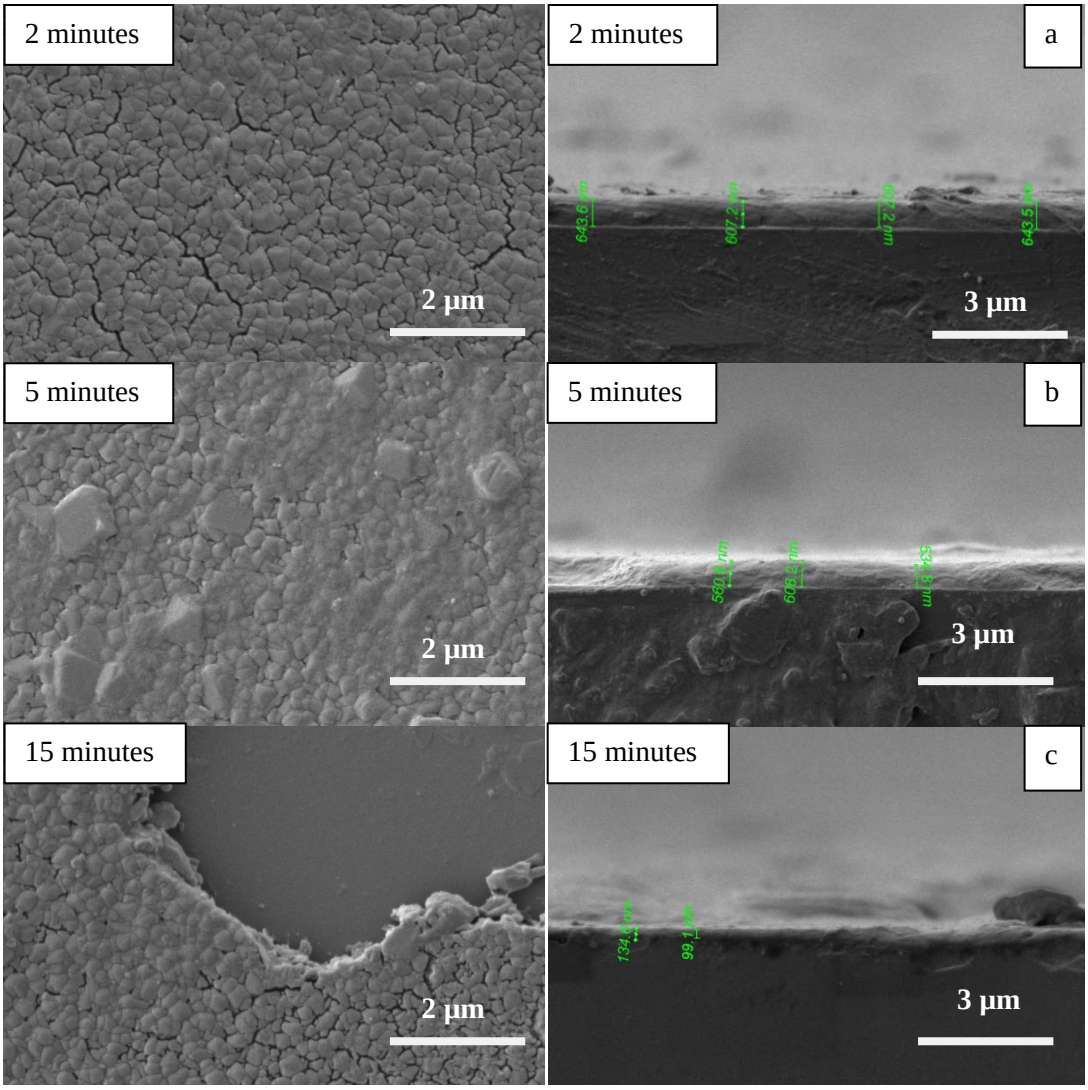

Figure 26 Comparison between ZIF-8 layers (top-view and cross-section view) after sonification in methanol for (a) 2 minutes, (b) 5 minutes and (c) 15 minute

- *Effect of acetone (with and without ultrasound) on ZIF-8 layer*

Acetone and ultrasound effect on ZIF-8 layer was tested to observe the adhesion of ZIF-8 layer on the silicon support and the stability of the layer during the lift-off process. The results are shown in Figure 23.

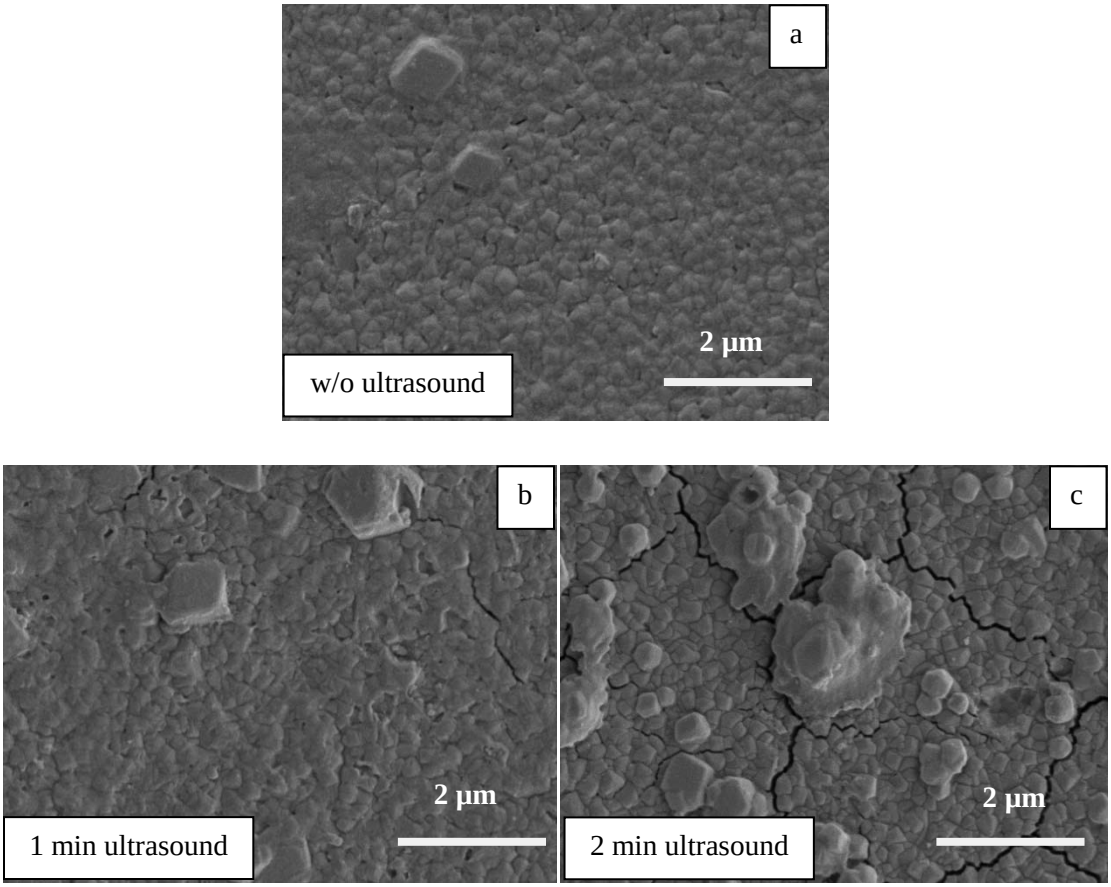

Figure 27 Effect of acetone to ZIF-8 layer (a) without sonication and with sonication for (b) 1 minute and (c) 2 minutes

Immersion of ZIF-8 layer in acetone (Figure 27(a)) does not affect the stability of the ZIF-8 layer. The effect of sonication in methanol and acetone shows the same phenomena which is the Ostwald ripening of ZIF-8 crystals on the layer.

ZIF-8 layer patterning by UV lithography

Based on the preliminary tests done for etching ZIF-8 layer and investigating the effect of acetone and ultrasound to the stability of the layer, UV lithography of ZIF-8

layer was done by RIE etching using O_2 plasma, and lift-off process using acetone without ultrasound treatment.

The result of UV exposure on ZIF-8 layer after development using AZ Developper solution is shown in Figure 28(a) where it can be seen clearly the pattern in which the black part was the photoresist which remained unexposed to the UV light. Positive photoresist (TI 35 ES) from Microchemicals consists of compounds of the diazonaphtho-quinone-sulphonates (DNQ) group, which transforms into carboxylic acid during UV exposure and become more soluble in basic solution, e.g. AZ developper solution.[79]

The positive resist deposition on the ZIF-8 layer had the thickness of around 2.5 µm, as measured by profilemeter. Photoresist is also etched by O_2 plasma in RIE process with an etching rate of ±1 µm/min. Therefore, etching of ZIF-8 layer was done for 10 minutes, to avoid complete etching of resist layer.

Lift-off process was done by washing with acetone and obtained pattern (Figure 28(b)) was observed using profilemeter by measurement of layer step between the etched and non-etched ZIF-8 layer. The thickness decrease is 559.4 nm that is more or less is in accordance to the etching rate obtained in preliminary RIE test, with a standard error of 4.67%.

Patterning ZIF-8 layer using UV lithography with a novel etching method by O_2 plasma RIE has been conducted successfully. The method can be implemented in the fabrication of ZIF-8 microcantilever sensors, as substitute for zeolite cantilevers [80] that require hydrothermal synthesis.

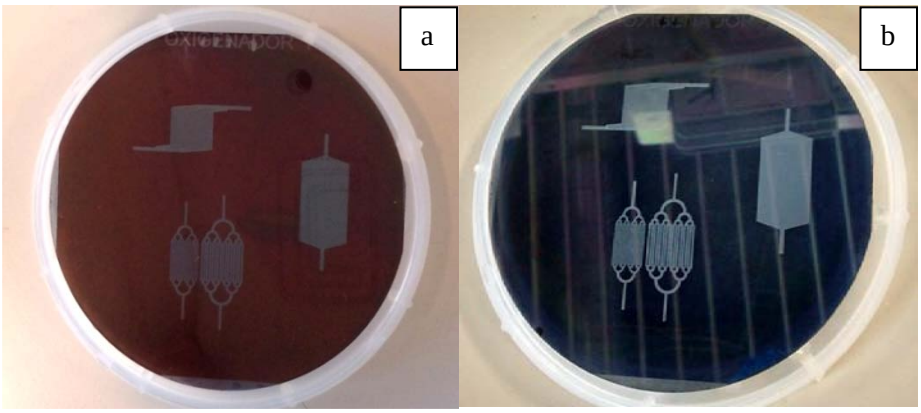

Figure 28 ZIF-8 layer patterning test (a) after revealing/development step and (b) final result after the lift-off step

4.1.4 ZIF-8 layer synthesis on patterned Si substrate

ZIF-8 layer synthesis in channels can be exploited for the purpose of fabricating a ZIF-8 based micro preconcentrator as a gas sensor enhancement. The procedure was begun by patterning the silicon wafer using RIE method with SF_6 plasma. SF6 plasma was chosen due to its reactivity with silicon wafers and rapid etching rate.[75]

Etched channels of ±30 µm depth are obtained after 30 minutes of etching. The positive resist remains attached on the layer and the synthesis of 20-cycle synthesis was conducted. The result after ZIF-8 layer synthesis and before lift-off process was observed using optical microscope and shown in Figure 29. Darker parts with black spots shows ZIF-8 layer grown on photoresist layer, and the light colored part was the ZIF-8 layer in the etched channel.

The obtained ZIF-8 layer shows non-homogeneity, especially seen by the different shades of colour accross the surface of the channel. The non-homogeneity is due to the existence of photoresist layer (organic compounds) which makes difference of the surface energy across the support. This induces growth of ZIF-8 crystals with a wide size distribution. Nevertheless, for the application of micro preconcentrator, non-homogeneity

of the layer can increase the performance of the device by increasing the amount of accessible surface area of the layer per total volume of gas mixture.

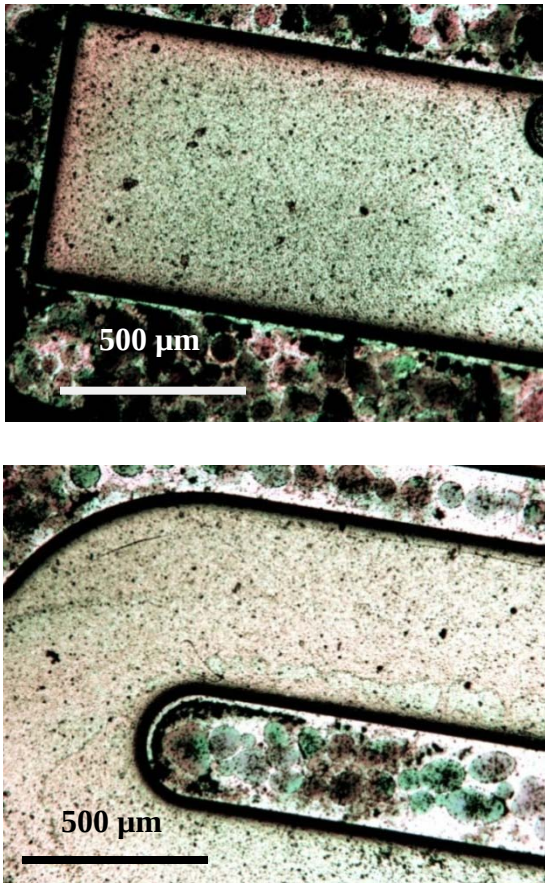

Figure 29 Two different parts of the ZIF-8 layer deposition on the photoresist layer and in the etched channel

The lift-off process was not successfully done by immersion in acetone neither with nor without ultrasound. This was due to the covering of photoresist layer by ZIF-8 layer which made it hard for the acetone to access the photoresist layer. Moreover, the adhesion of the ZIF-8 layer on the photoresist (organic material) surface is stronger than the one on the silicon support. Long exposure to sonication could induce faster removal

of ZIF-8 layer in the etched channel instead of the one on the photoresist layer. Therefore, photoresist lift-off was done mechanically by scratching using blade and rinsing with acetone.

Micro preconcentrator device packaging

In order for the deposited ZIF-8 layer can be fully integrated as a microdevice, the device should be closed by anodic bonding with Pyrex glass, shown in the process scheme in Figure 30.

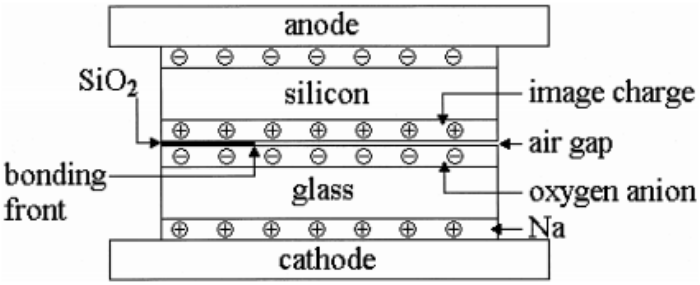

Figure 30 Cross-sectional view of anodic bonding process between silicon and glass materials [81]

Applied voltage and elevated temperatures will induce inmobile oxygen anions of the surface of the glass wafer. The interaction between the oxygen species and silicon surface would induce oxidation of the silicon species so that it would form thin layer of silicon oxide as bonding of both wafers. Therefore clean silicon wafer surface was very important to have good formation of silicon oxide thin layer and good closure of the device.[81] The result of closed ZIF-8 micro preconcentrator is shown in Figure 31.

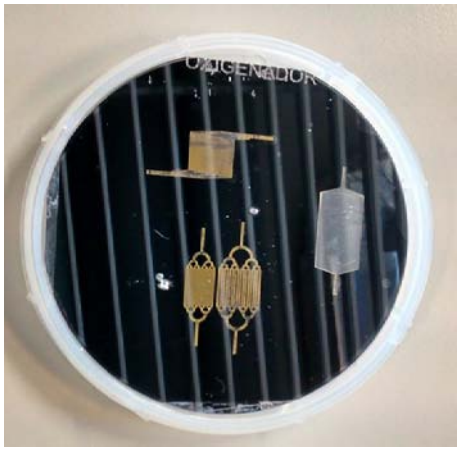

Figure 31 Closed ZIF-8 micro preconcentrator by anodic bonding with Pyrex glass

4.2 ZIF-8 layers on polymeric substrates

Based on the inability to build a free-standing ZIF-8 membrane on Si_3N_4 and SiO_2 grids and the known good adhesion of ZIF-8 crystals to polymeric materials, trials of ZIF-8 layer growth on polymeric substrates were conducted.

4.2.1 Growth of ZIF-8 layers on SU-8 substrates

Patterned SU-8 support can be obtained using soft lithography method, e.g. by molding.[81] Back-etching SU-8 support can be done according to developed RIE process using O_2 plasma.[83] Trials of ZIF-8 layer growth on the support was done based on good adhesion characteristic of ZIF-8 crystals to polymers and high thermal stability of both materials. Moreover, patterned support production does not involve photoresist deposition. Therefore, lift-off process that affects ZIF-8 crystal stability can be omitted.

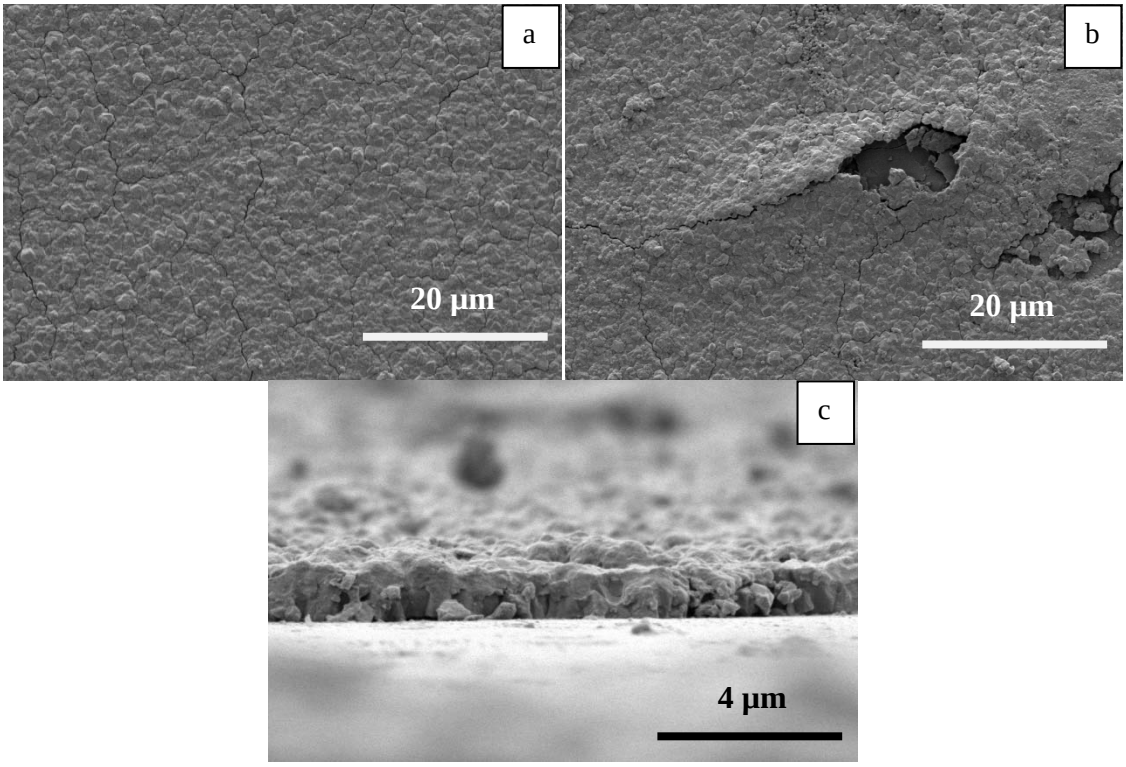

Figure 32 SEM top-view (above) and cross section (below) of ZIF-8 layer on SU-8 support after 20 cycles of synthesis

In Figure 32(a), it shows that the ZIF-8 layer has defects. Even though the width of the cracks is smaller, but lower crack-free surface area is obtained (compared to the layer on Si_3N_4 supports). Moreover, it also shows largely non-homogenous layer growth in Figure 32(b) and non-intergrown layer shown in the cross-section of the layer in Figure 32(c). The defects are hypothesized to be caused by slightly folding of the SU-8 support after the drying process in the synthesis. Therefore, the SU-8 supports cannot be utilized for ZIF-8 membrane fabrication.

4.2.2 Growth of ZIF-8 layers on porous PBI membranes

The experiments conducted for the growth of ZIF-8 layers on PBI membranes were firstly done in a small scale to test the compatibility of the synthesis method on both porous PBI membranes.

Small scale growth

The small-scale trial synthesis reveals that the porous asymmetric PBI membrane does not endure the ZIF-8 layer synthesis method. Rolled and very brittle membranes were obtained and shown in Figure 33, after 15 and 20 cycles of ZIF-8 layer synthesis.

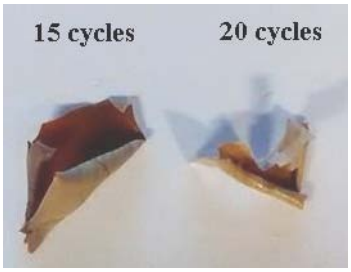

Figure 33 Resulted porous asymmetric PBI membrane after synthesis of ZIF-8 layers

On the other hand, the porous electrospunned PBI membranes remain in form during the synthesis, and SEM images of the samples from 10, 15 and 20 cycles of synthesis are shown in Figure 34.

The ZIF-8 layer does not grow on top of the PBI membrane surface; instead ZIF-8 crystals grow on the surface of the PBI fibers, due to the high porosity of the membrane so that the precursor molecules could diffuse inside the membrane. The good adhesion of the ZIF-8 crystals on the PBI fibers confirms the good compatibility between benzil-imidazole group in PBI and 2-methyl imidazole ligand of the ZIF-8 framework. Therefore crack-free deposition can be obtained (see Figure 34).

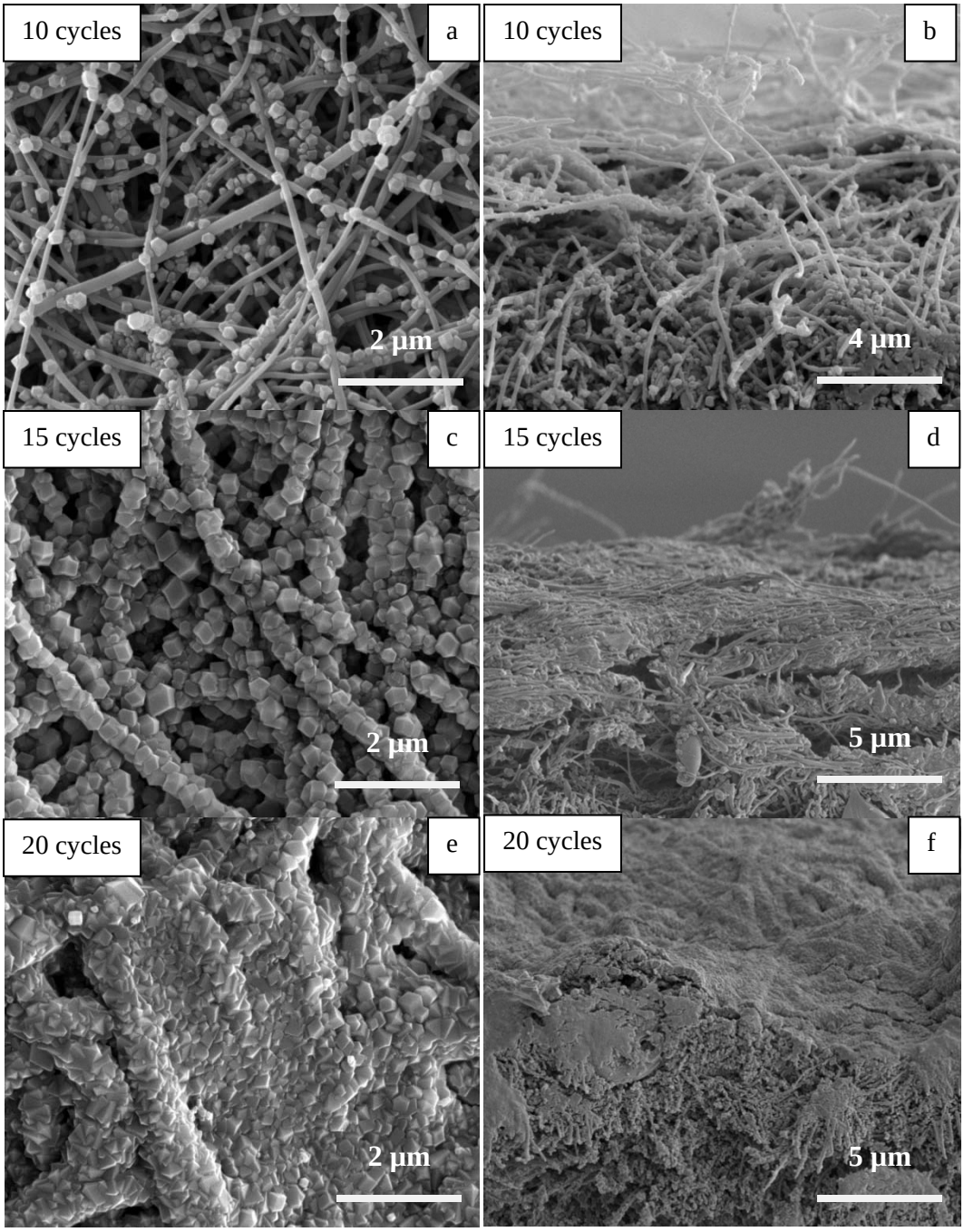

Figure 34 SEM top-view (left) and cross section (right) of ZIF-8 deposition on electrospunned PBI membrane for (a,b) 10 cycle, (c,d) 15 cycle and (e,f) 20 cycle of synthesis

As the number of synthesis cycle increases, the density of the hybrid membrane increases. After 20 cycle of synthesis, the ZIF-8 layer started to grow on the surface of the membrane which is already covered by ZIF-8 crystals. This is due to the less porosity of the composite membrane and selective ZIF-8 nucleation on the deposited ZIF-8 crystals.

Compared to PBI/ZIF-8 membrane obtained by Cacho-Bailo et al.[67], more deposition of ZIF-8 crystals were obtained inside the porous electrospunned PBI membrane, due to the high pore size of the PBI membrane. Moreover, the deposition of ZIF-8 layer was achieved on both sides of the PBI membrane (shown in Figure 35). Thicker ZIF-8 membrane (45 µm) was produced, compared to the 35 µm layer obtained by Cacho-Bailo et al. These results lead to denser membrane, i.e. more membrane retention and lower permeation flux.

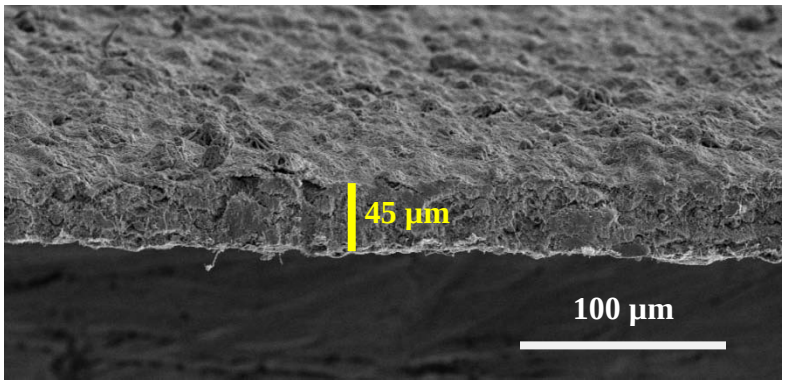

Figure 35 Cross section of PBI/ZIF-8 membrane from 20-cycle ZIF-8 layer synthesis

Up-scale growth

Based on the result of small scale trials, porous electrospunned PBI membrane was used. The stretching of the O-ring frame resulted to tear of the membrane on the edge part of the frame during the first cycle of the synthesis. Therefore, the synthesis was continued by direct immersion of the membrane without using stretcher (see Figure 36).

Figure 36 Final experimental set-up of big scale ZIF-8 synthesis on electrospunned PBI membrane

Although the electrospunned PBI membrane could remain stable throughout the ZIF-8 layer synthesis, the dry composite membrane also shows brittleness especially during the placement of the membrane in the membrane module of the permeation test. Therefore composite membrane for the application of hydrogen separation in high temperature and pressure condition cannot be achieved.

Distillation of methanolic waste solution from the synthesis and washing process of ZIF-8 layer growth, was successfully carried out in a more elevated temperature (110^{o}C) from the boiling point of methanol[84] due to the elevated pressure in the distillation system which induce the increase of methanol boiling point. After 3 cycles of distillation, clear methanol was obtained.

Synthesis of ZIF-8 layer for 15 numbers of cycles using distilled methanol produced layer deposition shown in Figure 37. The dots shown in the top view SEM image are caused by excessive Pt coating which was due to instable electrical current of the device. The thickness of the layer is less homogenous compared to the one obtained by utilizing anhydrous methanol due to impurities in the distilled methanol container and laboratory environment.

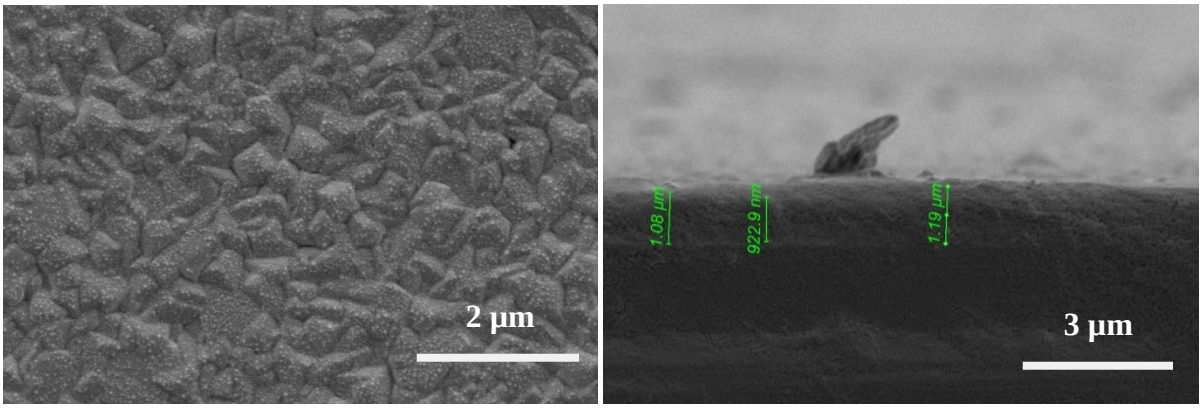

Figure 37 SEM images of ZIF-8 layer synthesized using distilled methanol

The crystallography of the obtained ZIF-8 layer was also tested using XRD analysis and the difractogram is shown in Figure 38. The difractogram peaks pattern obtained from synthesis using distilled methanol are identical with the synthesis with anhydrous methanol. The result also shows the same preferential crystal orientation into (110) direction.

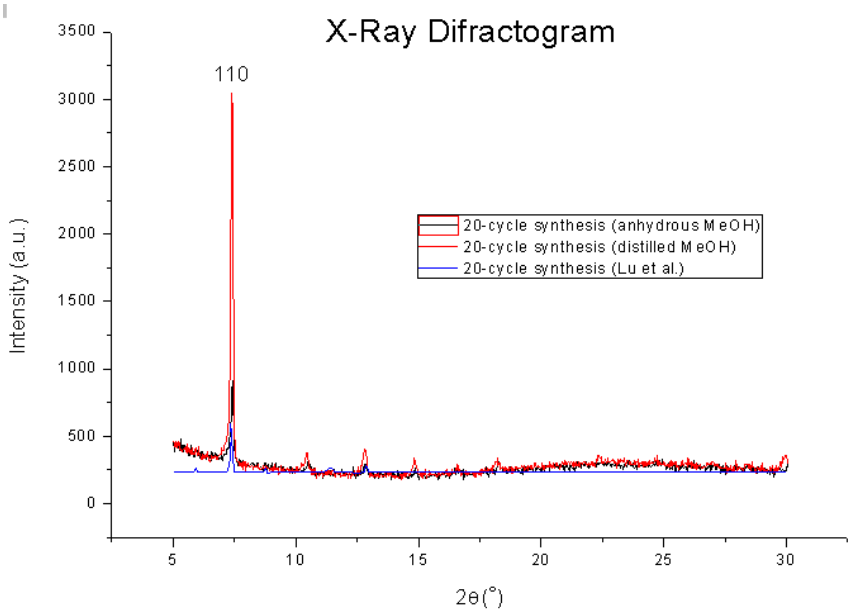

Figure 38 X-Ray difractogram of ZIF-8 layer experimental (using anhydrous and distilled methanol) and Lu et al.'s results

5. Conclusion and future work suggestions

In this Final Master Project, experiments on ZIF-8 layer integration in microdevices and membrane fabrication have been conducted. The tasks were divided into layer synthesis on different supports.

5.1 ZIF-8 layer on silicon based supports

ZIF-8 layer on silicon support

ZIF-8 layer on silicon support has been successfully synthesized, based on the synthesis method established by Lu et al.[55] The average layer thickness which can be obtained each cycle of synthesis is 68.6 nm. The ZIF-8 crystallography was confirmed by XRD and has the crystal orientation preference of (110).

Etching rate of ZIF-8 layer cannot be obtained from wet etching method using diluted HNO_3 solution. However, an etching rate 58.7 nm/min can be developed by Reactive Ion Etching (RIE) using O_2 plasma. Ultrasound has the effect of Ostwald ripening to the layer, creating defects such as cracks and layer detachment. The first goal of ZIF-8 layer patterning was successfully done by UV lithography method, incorporating O_2 plasma RIE for the etching step and acetone washing without ultrasound in the lift-off process. ZIF-8 layer pattern has a step thickness of 559.4 nm.

Results of ZIF-8 layer patterning shows that it is possible to pattern the layer by UV lithography, giving opportunity to exploit the layer in the application of microsensors. Future works in integration on ZIF-8 layer patterning in fabrication of ZIF-8 layer on microcantilevers and in its sensing ability can be carried out. Moreover, development of ZIF-8 layer synthesis inside micro continuous reactors by continuous precursor solution flow through the supports should be carried out in order to have a process that consumes less methanol and produces less waste.

ZIF-8 layer on patterned silicon support

ZIF-8 layer has been successfully grown on channel-shaped patterned silicon wafer. Lift-off process cannot be conducted by acetone washing, but is able to be carried out mechanically. The goal of integrating the ZIF-8 layer in micro preconcentrator was established by closing the device using anodic bonding with Pyrex glass. Future works in building device connections to adsorption test equipment and adsorption test of several gases can be carried out for the purpose of preconcentrator of low concentration analytes, in the range of ppt, such as explosives.

ZIF-8 layer on Si_3N_4 and SiO_2 supports

ZIF-8 layers on Si_3N_4 and SiO_2 supports show cracks. Etching rate of ZIF-8 layer KOH and TMAOH solutions is too high, resulting in complete reaction of the layer after 5 seconds exposure in the solutions. Therefore the goal of fabricating ZIF-8 layer as a free-standing micro membrane on Si_3N_4 and SiO_2 grids cannot be achieved. Future work on ZnO seed deposition before layer growing of ZIF-8 can be exploited to have better adhesion of the ZIF-8 layer on the Si_3N_4 and SiO_2 supports.

5.2 ZIF-8 layer on polymer based supports

ZIF-8 layer on SU-8 support

ZIF-8 layer on SU-8 support also shows cracks and nonhomogeneity. The goal of integrating ZIF-8 layer in free-standing micro membrane using SU-8 support cannot be achieved. Future experiments on experimental set-up improvements should be conducted in order to avoid SU-8 support folding during the synthesis and avoid cracking of the ZIF-8 layer.

ZIF-8 layer on porous PBI membranes

Porous asymmetric PBI membrane is too brittle to endure the synthesis of ZIF-8 layer. The porous electrospunned PBI membrane shows stability during the synthesis of the ZIF-8 layer. ZIF-8 crystals have good adhesion to the PBI fibers and the increase of synthesis' number of cycles increases the density of the membrane. The ZIF-8 crystals grow on both sides of the PBI support. Dry electrospunned-PBI/ZIF-8 composite membranes also show brittleness during the membrane placement in the membrane module of the permeation test set-up.

Future work in decreasing the brittleness of the composite membrane should be carried out. Synthesis of composite membranes using PBI support with smaller pore size should be investigated. Moreover, an experimental set-up needs to be developed to obtain one-side deposition of ZIF-8 layer, followed by permeation and selectivity of hydrogen gas in high temperature and pressure condition.

Reference

[1] Jensen, Klavs F., Silicon-Based Microchemical Systems: Characteristics and Applications. MRS Bulletin, 31, 2006, 101-107

[2] Asschem, Van, et al., Fabrication and separation performance evaluation of a metal–organic framework based microseparator device, Journal of Chemical Engineering Science, 95, 2013, 65–72

[3] Pellejero, Ismael, et al., Reinforced SIL-1 micromembranes integrated on chip: Application to CO_2 separation, Journal of Membrane Science, 460, 2014, 34 -45

[4] Devic, Thomas and Serre, Christian. (2009) Porous Metal Organic Frameworks : From Synthesis to Applications. In: Valtchev, V., et al. (eds.) Ordered Porous Solids. Elsevier B. V., page 78

[5] Wan, Yu Shan Susanna, et al., Design and fabrication of zeolite-based microreactors and membrane microseparators, Journal of Microporous and Mesoporous Materials, 42, 201, 157-175

[6] Pina, M. Pilar, Zeolite films and membranes. Emerging applications, Journal of Microporous and Mesoporous Materials, 144, 2011, 19-27

[7] Mohsen, Yehya , et al., Development of a micro-analytical prototype for selective trace detection of orthonitrotoluene, Microchemical Journal, 114, 2014, 48–52

[8] Pijolat, C., et al., Application of carbon nano-powders for a gas micro-preconcentrator, Sensor and Actuators B, 127, 2007, 179-185

[9] Blanco, F., et al, Fabrication and characterisation of microporous activated carbon-based pre-concentrators for benzene vapours, Sensors and Actuators B, 132, 2008, 90–98

[10] Leung, Yat Lai Adrian and K. L. Yeung, Microfabricated ZSM-5 zeolite micromembranes, Chemical Engineering Science 59, 2004, 4809–4817

[11] Coronas, J. and J. Santamaria, The use of zeolite films in small-scale and micro-scale applications, Chemical Engineering Science 59, 2004, 4809–4817

[12] Kreno, Lauren E., et al., Metal – Organic Framework Materials as Chemical Sensors, Chemical Reviews, 112, 2012, 1105 – 1125

[13] Liu, Jinxuan, et al. A novel series of isoreticular metal organic frameworks: realizing metastable structures by liquid phase epitaxy, Nature Scientific Reports, 2, 2012, 921.

[14] Meek, Scott T., et al., Metal – Organic Frameworks: A Rapidly Growing Class of Versatile Nanoporous Materials, Journal of Advanced Materials, 23, 2011, 249-267.

[15] Hermes, S., et al, Selective Nucleation and Growth of Metal–Organic Open Framework Thin Films on Patterned COOH/CF_3-Terminated Self-Assembled Monolayers on Au(111), Journal of American Chemical Society, 127, 2005, 13744-13745

[16] Qiu, Shilun, Ming Xue and Guangshan Zhu, Metal-organic framework membranes: from synthesis to separation application, Chemical Social Review Manuscript, 2013.

[17] Stock, Norbert and Shyam Biswas, Synthesis of Metal-Organic Frameworks (MOFs): Routes to Various MOF Topologies, Morphologies, and Composites, Chemical Review, 2012, 112, 933–969

[18] Li, Jian-Rong, Ryan J. Kuppler and Hong-Chai Zhou, Selective gas adsorption and separation in metal-organic frameworks, Chemical Social Review, 2009, 38, 1477-1504

[19] Thompson, Joshua A., et al., Hybrid Zeolitic Imidazolate Frameworks: Controlling Framework Porosity and Functionality by Mixed-Linker Synthesis, Chemistry of Materials, 2012, 24, 1930−1936

[20] Yao, Jianfeng , and Huanting Wang, Zeolitic imidazolate framework composite membranes and thin films: synthesis and applications, Chemical Social Review, 2014, 43, 4470

[21] Moh, Pak Y., et al., Crystallisation of solvothermally synthesized ZIF-8 investigated at the bulk, single crystal and surface level, Crystal Engineering Community, 2013, 15, 9672

[21] Park, K. S., et al., Exceptional chemical and thermal stability of zeolitic imidazolate frameworks, Proceedings of the National Academy of Sciences of the U. S. A., 2006, 103, 10186–10191.

[22] Huang, X. C. , J. P. Zhang and X. M. Chen, Chinese Scientific Bulletin, 2003, 48, 1531–1534.

[23] H. Bux, F. Y. Liang, Y. S. Li, J. Cravillon, M. Wiebcke and J. Caro, Zeolitic Imidazolate Framework Membrane with Molecular Sieving Properties by Microwave-Assisted Solvothermal Synthesis, Journal of the American Chemical Society, 2009, 131, 16000–16001

[24] Huang, X. C., Y. Y. Lin, J. P. Zhang and X. M. Chen, Angewandte Chemistry, International Edition, 2006, 45, 1557–1559.

[25] Hayashi, H. , A. P. Cote, H. Furukawa, M. O'Keefe and O. M. Yaghi, Nature Materials, 2007, 6, 501–506.

[26] Banerjee, R., A. Phan, B. Wang, C. Knobler, H. Furukawa, M. O'Keeffe and O. M. Yaghi, Science, 2008, 319, 939-943.

[27] Shah, M., H. T. Kwon, V. Tran, S. Sachdeva and H. K. Jeong, Microporous Mesoporous Materials, 2013, 165, 63–69.

[28] Banerjee, R., H. Furukawa, D. Britt, C. Knobler, M. O'Keeffe and O. M. Yaghi, Journal of American Chemical Society, 2009, 131, 3875–3877.

[29] Morris, W., C. J. Doonan, H. Furukawa, R. Banerjee and O. M. Yaghi, Journal of American Chemical Society, 2008, 130, 12626–12627.

[30] Wang, B., A. P. Cote, H. Furukawa, M. O'Keeffe and O. M. Yaghi, Nature, 2008, 453, 207–211.

[31] Aguado, S., C. H. Nicolas, V. Moizan-Basle, C. Nieto, H. Amrouche, N. Bats, N. Audebrand and D. Farrusseng, New Journal of Chemistry, 2011, 35, 41–44.

[32] Zhang, C. J., Y. L. Xiao, D. H. Liu, Q. Y. Yang and C. L. Zhong, Chemical Commununication, 2013, 49, 600–602

[33]Karagiaridi, Olga, Opening ZIF-8: A Catalytically Active Zeolitic Imidazolate Framework of Sodalite Topology with Unsubstituted Linkers, Journal of American Chemical Society, 2012, 134, 18790−18796

[34] Park, K.S., et al., Exceptional chemical and thermal stability of zeolitic imidazolate frameworks, Proceedings of the National Academy of Sciences of the United States of America, 103, 2006, 10186-10191

[35] Shah, Miral, et al., One step *in situ* synthesis of supported zeolitic imidazolate framework ZIF-8 membranes: Role of sodium formate, Microporous Mesoporous Materials, 2013, 165, 63–69

[36] Pan, Yichang and Zhiping Lai, Sharp separation of C2/C3 hydrocarbon mixtures by zeolitic imidazolate framework-8 (ZIF-8) membranes synthesized in aqueous solutions, Chemical Communications, 2011,47, 10275–10277

[37] Yao, J. F., L. X. Li, W. H. B. Wong, C. Z. Tan, D. H. Dong and H. T. Wang, Formation of ZIF-8 membranes and crystals in a diluted aqueous solution, Materials Chemistry and Physics, 2013, 139, 1003–1008.

[38] Tao, K., C. L. Kong and L. Chen, High performance ZIF-8 molecular sieve membrane on hollow ceramic fiber via crystallizing-rubbing seed deposition, Chemical Engineering Journal, 2013, 220,1-5

[39] Pan, Y.C., B. Wang and Z. P. Lai, Synthesis of ceramic hollow fiber supported zeolitic imidazolate framework-8 (ZIF-8) membranes with high hydrogen permeability, Journal of Membrane Science, 421–422, 2012, 292–298.

[40] Shekhah, O., R. Swaidan, Y. Belmabkhout, M. du Plessis, T. Jacobs, L. Barbour, I. Pinnau and M. Eddaoudi, The liquid phase epitaxy approach for the successful construction of ultra-thin and defect-free ZIF-8 membranes: pure and mixed gas transport study, Chemical Communications, 2014, 50, 2089–2092

[41] Ge, L., W. Zhou, A. J. Du and Z. H. Zhu, J. Phys. Chem. C,L. Ge, W. Zhou, A. J. Du and Z. H. Zhu, Porous Polyethersulfone-Supported Zeolitic Imidazolate Framework Membranes for Hydrogen Separation, Journal of Physical Chemistry C, 2012, 116, 13264–13270

[42] Ge, L., A. J. Du, M. Hou, V. Rudolph and Z. H. Zhu, Enhanced hydrogen separation by vertically-aligned carbon nanotube membranes with zeolite imidazolate frameworks as a selective layer, RSC Advances, 2012, 2, 11793–11800

[43] He, M., J. F. Yao, Z. X. Low, D. B. Yu, Y. Feng and H. T. Wang, A fast in situ seeding route to the growth of a zeolitic imidazolate framework-8/AAO composite membrane at room temperature, RSC Advances, 2014, 4, 7634–7639

[44] K. Huang, Z. Y. Dong, Q. Q. Li and W. Q. Jin, Growth of a ZIF-8 membrane on the inner-surface of a ceramic hollow fiber via cycling precursors, Chemical Communications., 49, 2013, 10326–10328

[45] M. C. McCarthy, V. Varela-Guerrero, G. V. Barnett and H. K. Jeong, Synthesis of Zeolitic Imidazolate Framework Films and Membranes with Controlled Microstructures, Langmuir, 26, 2010,14636–14641

[46] Tao, K., L. J. Cao, Y. C. Lin, C. L. Kong and L. Chen, A hollow ceramic fiber supported ZIF-8 membrane with enhanced gas separation performance prepared by hot dip-coating seeding, Journal of Material Chemistry A, 1, 2013, 13046–13049

[47] Xu, G.S., J. F. Yao, K. Wang, L. He, P. A. Webley, C. S. Chen and H. T. Wang, Preparation of ZIF-8 membranes supported on ceramic hollow fibers from a concentrated synthesis gel, Journal of Membrane Science, 385–386, 2011, 187–193

[48] Nagaraju, D., D. G. Bhagat, R. Banerjee and U. K. Kharul, In situ growth of metal-organic frameworks on a porous ultrafiltration membrane for gas separation, Journal of Material Chemistry A, 1, 2013, 8828–8835

[49] Li, L. X., J. F. Yao, R. Z. Chen, L. He, K. Wang and H. T. Wang, Infiltration of precursors into a porous alumina support for ZIF-8 membrane synthesis, Microporous Mesoporous Materials, 168, 2013, 15-18

[50] Zhang, X. F., Y. G. Liu, L. Y. Kong, H. O. Liu, J. S. Qiu, W. Han, L. T. Weng, K. L. Yeung and W. D. Zhu, A simple and scalable method for preparing low-defect ZIF-8 tubular membranes, Journal of Material Chemistry A, 1, 2013,10635–10638.

[51] Yao, J. F., D. H. Dong, D. Li, L. He, G. S. Xu and H. T. Wang, Contra-diffusion synthesis of ZIF-8 films on a polymer substrate, Chemical Commununication, 47, 2011, 2559–2561

[52] He, M., J. F. Yao, L. X. Li, Z. X. Zhong, F. Y. Chen and H. T. Wang, Aqueous solution synthesis

of ZIF-8 films on a porous nylon substrate by contra-diffusion method, Microporous Mesoporous Materials, 179, 2013, 10–16

[53] Xie, Z., J. H. Yang, J. Q. Wang, J. Bai, H. M. Yin, B. Yuan, J. M. Lu, Y. Zhang, L. Zhou and C. Y. Duan, Deposition of chemically modified a-Al2O3 particles for high performance ZIF-8 membrane on a macroporous tube, Chemical Communications, 48, 2012, 5977–5979

[54] Hara, N., M. Yoshimune, H. Negishi, K. Haraya, S. Hara and T. Yamaguchi, Diffusive separation of propylene/propane with ZIF-8 membranes, Journal of Membrane Science, 450, 2014, 215–223

[55] Lu, Guang and Joseph T. Hupp, Metal-Organic Frameworks as Sensors: A ZIF-8 Based Fabry-Perot Device as a Selective Sensor for Chemical Vapors and Gases, JACS, 132, 2010, 7832-7833

[56] Stassen, Ivo, Nicolo Campagnol, Jan Fransaer, Philippe Vereecken, Dirk De Vos, and Rob Amellot, Solvent-free synthesis of supported ZIF-8 films and patterns through transformation of deposited zinc oxide precurdors, Crystal Engineering Community,15, 20139308-9311

[57] Der Bruggen, Carlo Vandecasteele, Tim Van Gestel, Wim Doyen and Roger Leysen, A review of pressure-driven membrane processes in wastewater treatment and drinking water production Bart Van, 22, 2003, 46-56

[58] Kwon, H.T. and H. K. Jeong, In situ synthesis of thin zeolitic-imidazolate framework ZIF-8 membranes exhibiting exceptionally high propylene/propane separation, Journal of American Chemical Society, 135, 2013,10763-10768

[59] Falcaro, Pablo, et al., Patterning techniques for metal-organic frameworks, Advanced Materials, 2012, 3153 - 3168

[60] Li, Y. S., H. Bux, A. Feldhoff, G. L. Li, W. S. Yang, J. Caro, Advanced Materials, 22, 2010, 3322

[61] Ameloot, R., L. Stappers, J. Fransaer, L. Alaerts, B. F. Sels, D. E. De Vos, Chemical Communications, 46, 2010,3735

[62] Carbonell, C., I. Imaz, D. Maspoch, Journal of American Chemical Society, 133, 2013, 2144

[63] Lu, G., O. K. Farha, W. Zhang, F. Huo, J. T. Hupp, Engineering ZIF-8 Thin Films for Hybrid MOF-Based Devices, Advanced Materials, 24, 2012, 3970-2974

[64]Dimitrakakis, Constantinos, et al., Top-down patterning of zeolitic imidazolate framework composite thin films by deep x-ray lithography, 2, 2011, 237

[65] Microchemicals, SU-8 Permanent Photoresists – Technical Information, 2013, Microchemicals GmbH

[66] Yang, Tingxu and Tai-Shung Chung, High performance ZIF-8/PBI nano-composite membranes for high temperature hydrogen separation consisting of carbon monoxide and water vapor, International Journal of Hydrogen Energy, 38, 2013, 229-239

[67] Cacho-Bailo, F., B. Seoane, C. Tellez, J. Coronas, ZIF-8 continuous membrane on porous polysulfone for hydrogen separation, Journal of Membrane Science 464, 2014, 119–126

[68] Cubillas, P. and Anderson, M. W. (2010) Synthesis Mechanism: Crystal Growth and Nucleation, in Zeolites and Catalysis: Synthesis, Reactions and Applications (in eds J. Čejka, A. Corma and S. Zones), Wiley-VCH Verlag GmbH & Co. KGaA, Weinheim, Germany

[69] Tian, Fangyuan, et al., Surface and Stability Characterization of a Nanoporous ZIF-8 Thin Film, Journal of Physical Chemistry Manuscript, 2014.

[70] Cravillon, J. et al., Rapid Room-Temperature Synthesis and Characterization of Nanocrystals of a Prototypical Zeolitic Imidazolate Framework, Chemistry of Materials, 21, 2009, 1410-1412

[71] Bux, H., A. Feldhoff, J. Cravillon, M. Wiebcke, Y. S. Li, J. Caro, Oriented zeolitic imidazolate framework-8 membrane with sharp H_2/C_3H_8 molecular sieve separation, Chemistry of Materials, 23, 2011, 2262-2269

[72] Jaccodine, R J, Surface Energy of Germanium and Silicon". Journal of the Electrochemical Society 110, 1963, 524

[73] Critical Surface Tension, Surface Free Energy, Contact Angles with Water, and Hansen Solubility Parameters for Various Polymers, http://www.accudynetest.com/polytable_01.html, accessed June 9th 2014

[74] Pignataro, B., et al., Adhesion properties on nanometric scale of silicon oxide and silicon nitride surfaces modified by 1-octadecene, Surface and Interface Analysis, 33, 2002, 54-58

[75] Pellejero, I., M. Urbiztondo, M. Villarroya, J. Sese, M. P. Pina and J. Santamaria, Development of etching processes for the micropatterning of silicalite films, Microporous and Mesoporous Materials, 114, 2008, 110 – 120

[76] Altena, G. M. Dijkstra, H. J. W. M. Hoekstra and P. V. Lambeck, Ultra-thin free standing Si_3N_4 membrane waveguide for evanescent field sensing of MEMS movements, 12th European Conference of Integrated Optics, 2000, University of Twente, The Netherlands

[77] Chu, Ron F., 1996, Providing oxygen and water vapor into reaction chamber, sung radio frequency to excite and form plasma, US Patent 5567271A

[78] Thompson, Joshua A., Karena W. Chapman, William J. Koros, Christopher W. Jones, Sankar Nair, Sonication-induced Ostwald ripening of ZIF-8 nanoparticles and formation of ZIF-8/polymer composite membranes, Microporous and Mesoporous Materials 158 (2012) 292–299.

[79] Microchemicals, Exposure of Photoresist – Technical Information, 2013, Microchemicals GmbH

[80] Urbiztondo, M.A., I. Pellejero, M. Villarroya, J. Sesé, M.P. Pina, I. Dufour, J. Santamaría, Zeolite-modified cantilevers for the sensing of nitrotoluene vapors, Sensors and Actuators B: Chemical, 137, 2009, 608–616

[81] Lee, Thomas M.H., Debbie H.Y. Lee, Connie Y.N. Liaw, Alex I.K. Lao, I-Ming Hsing, Detailed characterization of anodic bonding process between glass and thin-film coated silicon substrates, Sensors and Actuators, 86, 2000, 103–107

[82] Cannistra AT, Suleski TJ, Characterization of hybrid molding and lithography for su-8 micro-optical components, Journal of Micro/Nanolithography, MEMS and MOEMS, 9, 2010, 13 – 25

[83] Rasmussen, K. H., S.S. Keller, F. Jensen, A.M. Jorgensen, O. Hansen, SU-8 etching in inductively coupled oxygen plasma, Journal of Microelectronic Engineering, 112, 2013, 35 – 40

[84] 322415 Sigma Aldrich – Methanol anhydrous 99.8% , http://www.sigmaaldrich.com/catalog/product/sial/322415?lang=es&region=ES, accessed June 23rd 2014

Appendix

1. Calculation of stoichiometric ZIF-8 layer thickness after 1 cycle of synthesis

ZIF-8 synthesis reaction

$$Zn(NO_3)_2 + 2\ mIm \rightarrow Zn(mIm)_2$$

Number of moles of the precursors in the solution

$$[Zn(NO_3)_2] = 25\ mmol/L = 0.025\ mol/L$$

$$\text{in 10 mL} \rightarrow n_{Zn(NO3)2} = 2.5 \times 10^{-4}\ mol$$

$$[mIm] = 50\ mmol/L = 0.05\ mol/L$$

$$\text{in 10 mL} \rightarrow n_{mIm} = 5 \times 10^{-4}\ mol$$

$$n_{Zn(mIm)2} = \underline{2.5 \times 10^{-4}\ mol}$$

Number of moles of the ZIF-8 in the layer of 1-cycle synthesis

$$\text{thickness } (\mu m) = 0.071 \text{ number of cycles}$$

$$1 \text{ cycle} \rightarrow \text{thickness} = 0.071\ \mu m$$

$$\text{Surface area} = 2 \times 2\ cm^2 = 4\ cm^2$$

$$V = 4\ cm^2 \times 0.071 \times 10^{-4}\ cm = 2.84 \times 10^{-5}\ cm^3$$

$$\rho_{ZIF\text{-}8} = 0.35\ g/cm^3 \text{ (Sigma-Aldrich)}$$

$$m_{ZIF\text{-}8} = 0.35\ g/cm^3 \times 2.84 \times 10^{-5}\ cm^3 = 9.94 \times 10^{-6}\ g$$

$$Mr_{ZIF\text{-}8} = 229.6\ g/mol \text{ (Sigma-Aldrich)}$$

$$n_{ZIF\text{-}8} = 9.94 \times 10^{-6}\ g : 229.6\ g/mol = \underline{4.33 \times 10^{-8}\ mol}$$

ZIF-8 layer thickness based on stoichiometric calculation

$$\text{thickness} = \frac{2.5 \times 10^{-4}}{4.33 \times 10^{-8}} \times 0.71\ \mu m = 409.93\ \mu m = 0.41\ mm$$

Stoichiometrically, 1-cycle synthesis precursors can form a layer of 0.41 mm.

2. Calculation of Surface-to-volume ratio of silicon wafer, PA and PTFE containers in the precursor solution

Surface- to-volume ratio (S/V) of a silicon wafer in the precursor solution:

diameter (d) = 7.5 cm ; r = 3.75 cm

S = πr^2 = 44.1 cm^2

$V_{solution}$ = 100 mL

$S/V_{silicon}$ = 0.44 cm^2/mL

Surface-to-volume ratio (S/V_{PTFE}) of immersed surface of round PTFE container:

diameter (d) = 7.5 cm; r = 3.75 cm

height of the precursor solution in the container ($h_{immersed}$) = 3 cm

S :

- base = πr^2 = 44.1 cm^2
- sides = $\pi d h_{immersed}$ = 70.65 cm^2

S = 114.75 cm^2

$V_{solution}$ = 100 mL

S/V_{PTFE} = 1.15 cm^2/mL

Surface-to-volume ratio (S/V_{PA}) of immersed surface of square PA container:

square size (w) = 10 cm

thickness (t) = 3 cm

S = 2ww + 2wt = 200 + 60 = 260 cm^2

$V_{solution}$ = 100 mL

S/V_{PA} = 2.6 cm^2/mL